Joni Malén

Analysis of noise emissions of solar inverters

School of Electrical Engineering

Thesis submitted for examination for the degree of Master of Science in Technology.

Helsinki September 23, 2013

Thesis supervisor:

Prof. Vesa Välimäki

Thesis instructor:

D.Sc. (Tech.) Janne Roivainen

Aalto University
School of Science
and Technology

AALTO UNIVERSITY
SCHOOL OF SCIENCE AND TECHNOLOGY

ABSTRACT OF THE
MASTER'S THESIS

Author: Joni Malén

Title: Analysis of noise emissions of solar inverters

Date: September 23, 2013 Language: English Number of pages:9+75

School of Electrical Engineering

Department of Signal Processing and Acoustics

Professorship: Audio Signal Processing Code: S-89

Supervisor: Prof. Vesa Välimäki

Instructor: D.Sc. (Tech.) Janne Roivainen

Frequency converters and solar inverters are becoming more commonplace, yet there is little to no literature concerning their noise emissions or noise generation mechanisms. There neither exists a standard procedure to measure or to verify their noise emissions. This thesis aims to rectify this situation.

Eight on-market solar inverters were examined to find their noise emissions and the voltage- and power-related variability in those noise emissions. Additionally, a Generic Device was partially disassembled to reveal the contributions of various noise sources.

All measured devices exhibit a positive correlation between operating power and noise emission. Conversely, no such correlation exists between operating voltage and noise emission. The cooling fan is responsible for the majority of noise emission below 10 kHz, whereas the chokes are the major sources of noise above 10 kHz. For the majority of devices, noise above 10 kHz represents a significant portion of total noise, and must be included in sound power measurements. Emission sound pressure levels exhibit great variability in space and thus must be determined empirically at specified positions.

Keywords: frequency converter, solar inverter, audible noise, noise analysis, noise control

AALTO-YLIOPISTO
TEKNILLINEN KORKEAKOULU

DIPLOMITYÖN
TIIVISTELMÄ

Tekijä: Joni Malén

Työn nimi: Aurinkosähkövaihtosuuntaajien melupäästöjen analyysi

Päivämäärä: September 23, 2013 Kieli: Englanti Sivumäärä:9+75

Sähkötekniikan korkeakoulu

Signaalinkäsittelyn ja akustiikan laitos

Professuuri: Äänisignaalinkäsittely Koodi: S-89

Valvoja: Prof. Vesa Välimäki

Ohjaaja: TkT Janne Roivainen

Taajuusmuuttajat ja aurinkosähkölaitteet yleistyvät, mutta ei ole olemassa kirjallisuutta koskien niiden melupäästöjä eikä niiden melunsyntymekanismeja. Myöskään ei ole olemassa standardoitua menetelmää niiden melupäästöjen mittaamiseksi tai todentamiseksi. Tämän opinnäytteen tarkoituksena on paikata tätä vajetta.

Kahdeksan markkinoilla olevaa aurinkosähkömuuttajaa tutkittiin niiden melupäästöjen selvittämiseksi. Lisäksi tutkittiin melupäästöjen riippuvuutta laitteen käyttöjännitteestä ja -tehosta. Näiden lisäksi tyypillinen laite purettiin osittain taajuusmuuttajien melunlähteiden selvittämiseksi.

Kaikilla mitatuilla laitteilla havaittiin positiivinen riippuvuussuhde laitteen käyttötehon ja melupäästön välillä. Sen sijaan laitteiden käyttöjännitteen ja melupäästön välillä ei havaittu selvää riippuvuussuhdetta. Laitteiden jäähdytyspuhallin vastaa pääosasta laitteiden melupäästöä 10 kHz:a pienemmillä taajuuksilla, kun taas laitteen kuristin on tärkein melulähde 10 kHz:n yläpuolella. Valtaosalla laitteista 10 kHz:n yläpuolinen taajuusalue on merkittävä osa kokonaismelupäästöä, ja se tulee sisällyttää kaikkiin äänitehomittauksiin. Päästöäänenpainetasoissa havaittiin merkittäviä paikkariippuvaisuuksia, ja ne tulee määrittää empiirisillä mittauksilla erikseen määritellyissä paikoissa.

Avainsanat: taajuusmuuttaja, aurinkosähkövaihtosuuntaaja, melu, meluanalyysi, meluntorjunta

Acknowledgements

This thesis certainly was not without its obstacles. I would first like to thank both my instructor, Janne Roivainen, and my supervisor, Vesa Välimäki, for enduring through this process to its conclusion.

Second, I would like to thank Antti Kuhlberg for providing invaluable assistance in the measurements. Without your help, I don't think this thesis would have been a reality. Another thesis, perhaps, but not *this* one.

Third, I would like to thank Merita Petäjä for guiding me through this process and helping me persevere in circumstances I at times thought unbearable.

Fourth, I would like to thank my family for always being there. Thanks also go to my friends and fellow students for understanding and supporting me in the course of this work, no matter how absurd things became.

Finally, and most importantly, I offer my sincerest love and gratitude to my partner, Kati, for her unwavering support in the face of any and every obstacle life put in our path. You are the reason I kept going.

Otaniemi, September 23, 2013

Joni Malén

Contents

Abstract ii

Abstract (in Finnish) iii

Acknowledgements iv

Contents v

Symbols and abbreviations viii

1 Introduction 1

1.1 Research questions 1

1.2 Structure of this thesis 2

2 Basics of frequency converters and solar inverters 3

2.1 Electrical operation of frequency converters 3

2.2 Assumed noise sources 5

3 Basics of noise generation 7

3.1 Preliminaries of acoustic field theory 7

3.2 Sources of sound 9

3.3 Structural acoustics 11

3.4 Sound generation in axial flow fans 13

3.5 Sound generation in chokes 15

4 Acoustic research methods and equipment 16

4.1 Acoustic research equipment 16

4.1.1 Microphones 16

4.1.2 Sound intensity probes 17

4.1.3 Sound calibrators 18

4.1.4 Sound level meters 19

4.1.5 Reference sound sources 19

4.2 Measurement standards 20
4.2.1 Standards for the determination of sound power 21
4.2.2 Standards for the determination of emission sound pressure levels 22
4.2.3 Standards on noise test codes 23
4.2.4 Standards concerning the presentation of noise levels 25

5 Presenting the test case 27

5.1 Devices to be tested 27
5.2 Choice of method 27
5.2.1 Determining sound power levels via ISO 3744 28
5.2.2 Determining sound pressure levels via ISO 11203 35
5.3 Testing facilities and equipment assembly 37
5.4 Measurement equipment 38
5.5 The testing plan 38

6 Research results 40

6.1 Preliminary measurements 40
6.1.1 Background noise 40
6.1.2 Reference sound source 40
6.2 Generic Device 42
6.2.1 Generic Device with choke assembly 42
6.2.2 Generic Device without choke assembly 42
6.2.3 Choke assembly only 43
6.3 On-market devices 46
6.3.1 Danfoss TLX 15 46
6.3.2 Fronius IG TL 5.0 47
6.3.3 Kostal PIKO 8.3 47
6.3.4 PowerOne Aurora Trio 20.0 47
6.3.5 PowerOne PVI-3.0 49
6.3.6 REFUsol 017K 49

6.3.7 SMA Sunny Tripower 6000TL 49
6.3.8 Voltwerk VS 15 51

7 Analysis of results **53**
7.1 Validity of results 53
7.2 Noise source analysis of Generic Device 53
7.2.1 Noise component analysis 53
7.2.2 Voltage-related variability of noise emission 55
7.2.3 Power-related variability of noise emission 57
7.3 Noise emissions of on-market devices 59
7.3.1 Congruence with declared noise emission values 59
7.3.2 Voltage-related variability of noise emissions 60
7.3.3 Power-related variability of noise emissions 65

8 Conclusions and suggestions **69**
8.1 Suggestions for noise emission declarations for solar inverters 70
8.2 Suggestions for dealing with cooling fan and choke noise 70
8.3 Suggestions for further research 71

Symbols and abbreviations

Symbols

B	bulk modulus
d	measurement distance, separation distance
d_O	characteristic dimension of noise source
D_I^*	apparent directivity index
f	frequency
G	cross spectrum
k	coverage factor
K_1	background noise correction term
K_2	environmental correction term
l	length
L_W	unweighted sound power level
L_{WA}	A-weighted sound power level
$L_{WA,f}$	A-weighted sound power level at frequency f
$L_{WA,ext}$	A-weighted sound power level with extended bandwidth
$\overline{L_p}$	corrected surface time-averaged sound pressure level
$\overline{L'_p}$	uncorrected mean time-averaged sound pressure level
L'_p	uncorrected time-averaged sound pressure level
p	sound pressure
p_0	reference sound pressure
Q	sound power level to emission sound pressure level determination quantity
r	measurement radius
S	measurement surface area
S_0	reference surface area
$\bar{u}$	particle velocity
U	uncertainty
V_I^*	apparent surface sound pressure level non-uniformity index
σ	standard deviation
ω	angular frequency

Abbreviations

AC	alternating current
B&K	Brüel & Kjær
BPF	blade passing frequency
DC	direct current
DUT	device under test
ECMA	European Computer Manufacturers' Association (deprecated)
GD	Generic Device
HP	Hewlett-Packard
IEC	International Electrotechnical Commission
IGBT	insulated gate bipolar transistor
ISO	International Organization for Standardization
PWM	pulse-width modulation
RMS	root mean square
RSS	reference sound source
TC	Technical Committee

1 Introduction

Solar power represents a major avenue of energy production going into the future. As the usage of fossil fuels is intended to decline, there arises a need for cleaner alternatives. Solar power is an obvious choice. Daily insolation of the Earth's surface provides enough energy to power all of humanity for a full year. Solar irradiation provides so much energy, in fact, that a meager 3% of desert lands could provide for all the world's energy needs, even using today's solar panel technology. And solar panels are improving all the time. (Blazev, 2012)

All this solar energy generation mandates a new energy grid and technology to transfer energy from the panels to the grid. Solar inverters are just the device for that. As solar inverters become more and more commonplace, their environmental impacts become all the more significant. Among these impacts is noise, particularly audible noise. Audible noise can range from a minor annoyance to a source of permanent injury to the ears. So far, there have been limited forays into the exploration of noise generation in solar inverters.

This thesis addresses exactly that. In this thesis, noise emissions of eight on-market devices of varying power ratings are measured. In addition, a Generic Device, provided by ABB is disassembled and run at varying configurations to discern the noise impacts various components. Finally, a standardized measurement protocol is suggested to accurately reflect the noise emissions of this family of devices.

1.1 Research questions

This thesis is intended to explore three questions:

1. What are typical noise emission levels of on-market solar inverters?
2. Do these devices' noise emissions exhibit variations due to different voltage or power levels?
3. How much noise is due to the cooling fans, how much due to chokes, and how much due to everything else?

To accomplish the first two goals, an array of extant devices were selected for measurement. These devices were run at various operating points. To accomplish the third goal, a frequency converter similar to the solar inverters was provided by ABB. The device, henceforth referred to as the Generic Device (GD), underwent significant modifications to separate assumed noise sources.

1.2 Structure of this thesis

This thesis is divided into eight sections. In Section 1, the goals of this thesis are presented. In Section 2, solar inverters are introduced. Section 3 introduces acoustic preliminaries necessary to understanding this thesis. Section 4 presents a comprehensive overview on standards pertaining to the measurement of sound emissions. Section 5 presents the process used to measure the devices. Test results are presented in Section 7. The thesis is concluded in Section 8.

2 Basics of frequency converters and solar inverters

A *frequency converter* is a power electronic device that changes the input frequency of a power signal to the output frequency with minimal losses in power. This allows for machines such as motors and generators to run at a frequency suited to the task (operating pumps or conveyor belts, for instance) on a power supply or power output whose frequency is constant, such as 50 or 60 Hz mains grids, without the need for elaborate gear systems. All conversion between frequencies is done by signal processing means with power electronic components.

A *solar inverter* is a special case of a frequency converter, in that the input source is assumed to come from *solar panels*. A solar panel is an array of *solar cells*, which generate DC currents from solar radiation via the *photovoltaic effect* (Blazev, 2012). Thus, the input signal does not need to be rectified, and only the output signal needs to be generated. Solar inverters are typically used to generate electricity and to "feed" the mains grid, so that the grid operator remunerates the user for the electricity generated.

2.1 Electrical operation of frequency converters

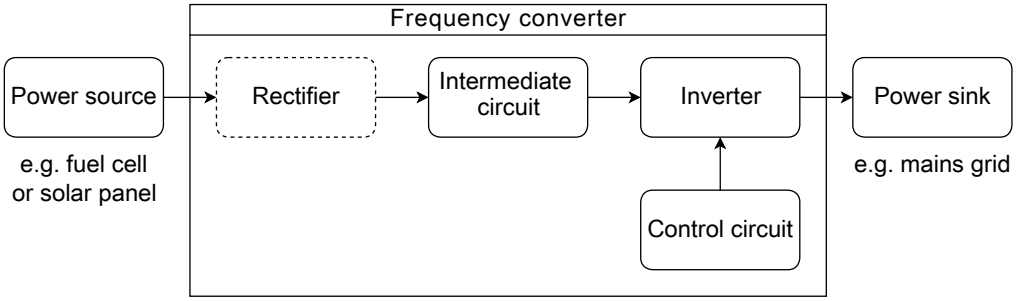

Figure 1: Generalized block diagram of a frequency converter. In solar inverters, the rectifier stage is optional and often unnecessary.

A general frequency converter consists of a rectifier stage, an intermediate circuit, and an inverter stage (Figure 1). A solar inverter is a special case, where the rectifier stage is unnecessary, since the input is considered to be essentially a DC signal. Another peculiarity of solar inverters is that the output frequency is typically stationary at the grid frequency, e.g. 50 or 60 Hz. This greatly reduces the complexity required of the control circuit. (Erkinheimo et al., 1997)

The input stage of frequency converters typically consists of a diode bridge for rectification (thyristors can also be used). The bridge consists of a pair of diodes for each phase of input current.

The intermediate circuit serves to regulate either the current or the voltage of the DC stage, depending on design choices, and usually consists of a high-power inductor known as a *choke*, and optionally of a capacitor, when dealing with voltage-based intermediate circuits (Niiranen, 1999). All these components serve to reduce the AC components in the pre-inverter stage.

The inverter stage of a frequency converter consists of *DC choppers* that serve essentially as switches. In high-power applications, these components are typically thyristors or *insulated gate bipolar transistors* (IGBTs). By turning them on and off in a specific fashion, a semblance of sinusoidal output current is achieved.

Pulse-width modulation (PWM) is a modulation technique where a rectangular waveform with varying duty cycle is used to control the conductivity of the DC choppers. In the case of sinusoidal signals, as is the case here, a desired sine wave *(utility signal)* of frequency f_u is compared against a triangular wave of higher frequency f_c *(carrier signal)*, as illustrated in Figure 2. When the amplitude of the utility signal is higher than the amplitude of the carrier signal, the choppers are conductive (Figure 3). A control circuit is used to generate these waveforms, and the analogue signals are fed to a comparator, which in turn serves as the control signal for the DC choppers. (Niiranen, 1999; Thorborg, 1988; Shireen et al., 2006)

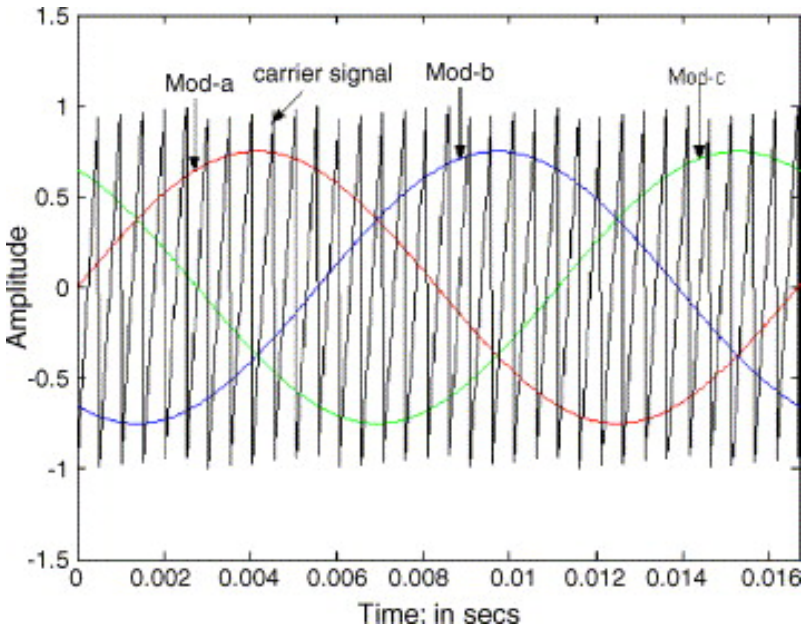

Figure 2: Comparison of sinusoidal utility signals and a triangular carrier. $f_u = 60$ Hz and $f_c = 1980$ Hz. Taken from Shireen et al. (2006).

The resulting frequency spectrum of PWM is one where there are peaks at the utility signal frequency and its harmonics, and a *sinc* type distribution with peaks spaced f_u apart centered around f_c and its harmonics (Figure 4). (Shireen et al., 2006)

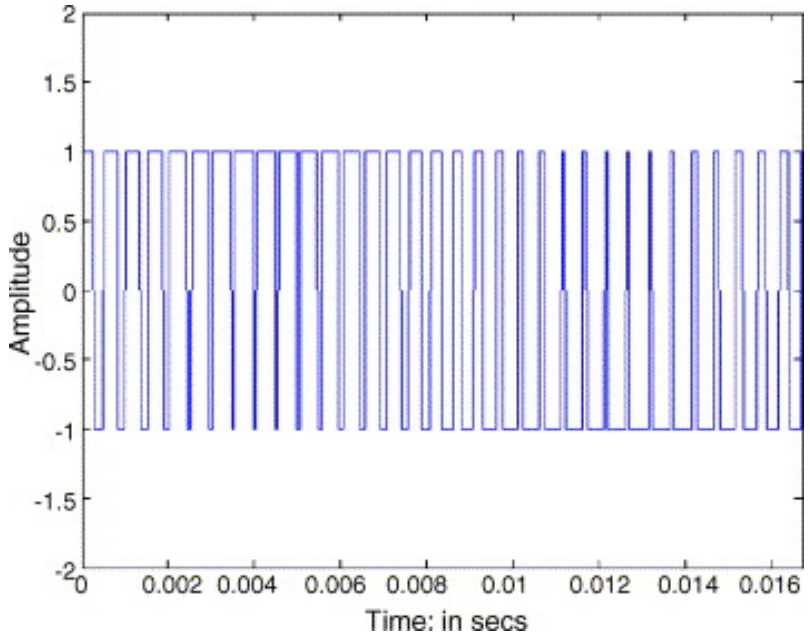

Figure 3: PWM switching function. $f_u = 60$ Hz and $f_c = 1980$ Hz. Taken from Shireen et al. (2006).

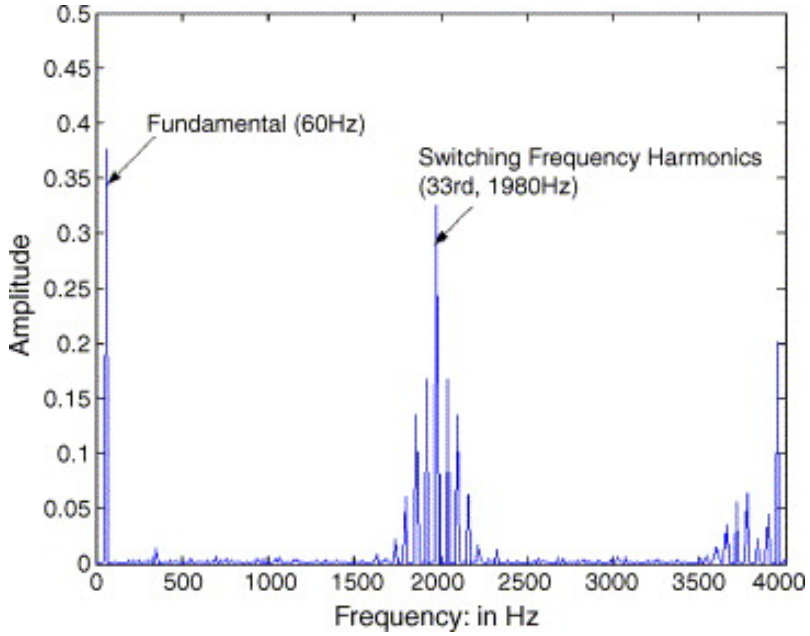

Figure 4: Spectrum of PWM switching function. $f_u = 60$ Hz and $f_c = 1980$ Hz. Taken from Shireen et al. (2006).

2.2 Assumed noise sources

In order for a component to act as a noise source, it needs to dissipate some of the energy flowing through it into mechanical vibration of the supporting structures or

of the surrounding air itself. Based on field experience, it was assumed that the noise was primarily due to cooling fans. Also, as the choke inductors act basically as low-pass filters on the electric signal, they dissipate significant energies on the "ripple" of the intermediate circuit current. Audible noise is a common problem in power inductors (Thorborg, 1988). According to John J. Winders (2002), "essentially all transformer noise is due to a phenomenon called magnetostriction", and since a transformer is essentially a coil array with a shared core, the origin of electromagnetic noise can be quite safely assumed to be similar.

Frequency converters and solar inverters are high-power devices, and as such, even minor power losses can generate significant heat. Thus, these devices need to be cooled. Some devices can be water cooled, but the vast majority of devices are air cooled. Fans can generate significant audible noise, and the noise output is directly related to airflow requirements.

A frequency converter can operate at various voltages and electrical powers. To investigate whether the devices exhibit voltage- or power-dependent noise emissions, the devices were run at various voltages and various power outputs at each voltage.

3 Basics of noise generation

In order to understand the phenomenon of noise and the means by which we aim to suppress it, we must first explore the nature of sound as a physical phenomenon, and the tools and methods we have to explore these physical phenomena.

3.1 Preliminaries of acoustic field theory

Sound, at its essence, is both the vibration of a medium and the human perception of it. The quality that humans perceive is the pressure of sound at perceivable frequencies. While physical vibrations can exist at virtually all frequency and pressure levels, humans can only perceive a limited spectrum of it. It is nominally accepted that humans can perceive frequencies of sound within 20 Hz and 20 kHz, although most people fall short on either end, and a select few can perceive sounds outside this range.

The lowest and highest perceivable sound pressure levels at which sounds exist are somewhat more complex, as it depends both on the sound pressure level itself, and of the frequency where it resides. The quantity of perceived amplitude of sound is called *loudness* and its unit is the *phon*. The sound pressure levels for which sounds at different levels are perceived to be the same, are illustrated by a series of graphs known as *equal-loudness contours*, and are specified in ISO 226 (1987). These contours are illustrated in Figure 5.

Sound pressure is the force per unit area which molecules in a medium produce as a manifestation of the change in momentum these particles undergo as a result of particle-particle interactions (Fahy, 2001). The pressure extant in a volume of medium is dependent on both the density and the temperature of the medium in an adiabatic (i.e. non-linear) fashion, but for most practical purposes, the linearization of the process yields negligible errors.

The consideration of sound pressure alone would yield only locally limited sound fields, but in order to study noise, we must also consider the propagation of sound. When sound flows from one place to another, it exhibits *particle velocity* dependent on pressure differences, as characterized by the equation

$$\nabla p = -\rho_0 \frac{\partial \bar{u}}{\partial t}, \tag{1}$$

where p is sound pressure, ρ_0 is the static density of the medium, $\bar{u}$ is the particle velocity and t is time. Similarly,

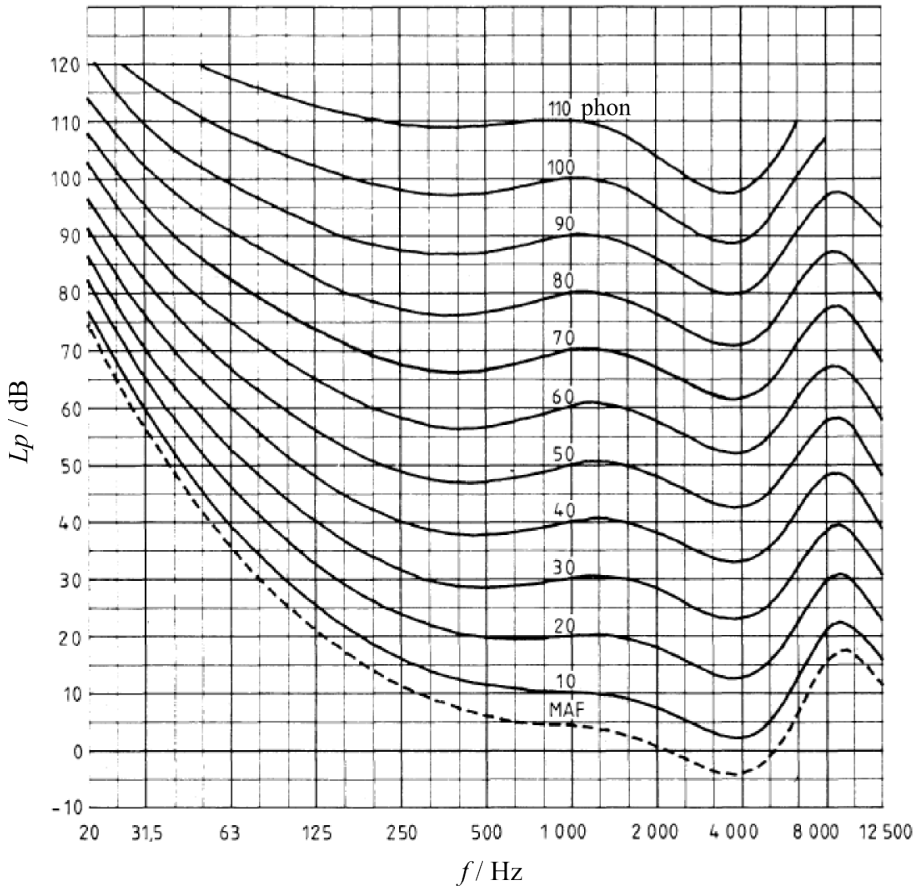

Figure 5: Equal-loudness contours of human hearing. MAF = minimal auditory field. (ISO 226, 1987)

$$\nabla \cdot \bar{u} = -\frac{1}{B}\frac{\partial p}{\partial t}, \tag{2}$$

where B is the bulk modulus of the medium. (Fahy, 2001; Lahti, 2009)

Thus, we have characterized the two fundamental acoustic qualities — sound pressure and particle velocity — as they exist in a medium. Also, we have characterized the medium with regard to two acoustically significant properties: its density and its bulk modulus. The ratio of these quantities yields the speed of sound in the medium as per

$$c^2 = \frac{B}{\rho_0}, \tag{3}$$

where c is the speed of sound. Thus, we can define the *characteristic acoustic impedance* of a medium as

$$Z_0 = \rho_0 c = \rho_0 \sqrt{\frac{B}{\rho_0}} = \sqrt{B\rho_0}. \tag{4}$$

Therefore, we can define *sound energy* as the mechanical energy extant per unit volume. It reduces to kinetic energy associated with sound, dependent on particle velocity, and potential energy associated with sound, dependent on sound pressure. Concisely,

$$E_{sound} = \frac{1}{2}\rho_0 |\bar{u}|^2 + \frac{1}{2}\frac{p^2}{B}. \tag{5}$$

Sound energy is important in that it allows us to inspect flow of acoustic energy between regions whose energies differ. *Sound intensity* is the quality by which flow of sound energy is inspected, and is defined as the time rate of work per unit area, or

$$\bar{I} = \frac{\mathrm{d}W}{\mathrm{d}t}\frac{1}{\delta\bar{S}} = p\bar{u}, \tag{6}$$

where $\bar{I}$ is sound intensity, W is work performed and $\delta\bar{S}$ is an area element vector. Because sound intensity represents flow of sound energy between regions, we can define the *emission sound power* of a source as the sum of radiated sound intensity, or total work performed per unit time. This reduces to

$$P = \int_S \bar{I} \cdot \mathrm{d}\bar{S}, \tag{7}$$

where S is a closed surface enveloping the source being inspected.

3.2 Sources of sound

When analyzing sound emissions, the source can be characterized in a number of ways:

- The phenomenological basis of sound generation
- The radiation pattern
- Time characteristics of emission
- Spectral characteristics of emission

The phenomenological characterization of sources groups them into three categories. The first category involves volume fluctuations, wherein the source actively displaces a volume of fluid, thus causing a volume acceleration. An example of this category is a loudspeaker cone that "pushes" air. Category 2 sources, on the other hand, involve forces that are time-varying, but do not cause net displacements of air. An example of this is the vortex shedding phenomenon of fans, where the boundary layer between the air and the blade moves at speeds approaching the velocity of the blade, while air is effectively stationary further from the blade. This creates differences in pressure and particle velocity, which in turn cause sound to propagate from the blades. Category 3 sources involve neither net volume displacements nor net forces. An example of this is the case of clacking billiard balls, where the accelerations of the balls are equal and opposite. The generation of sound is by the boundary layers of fluid travelling and decelerating with the balls. (Fahy, 2001)

The second categorization of sources is due to radiation pattern. The simplest acoustic source is an acoustic monopole that takes the form of an elementary sphere, whose radius contracts and expands uniformly in all dimensions. Thus, there exist time varying pressure fluctuations that are solely dependent on the distance from the center of the sphere. An acoustic dipole consists of two monopoles in close proximity vibrating in opposite phase. Thus radiation is equal but opposite on the axis of connection and zero perpendicular to said axis. Further examples of radiators, such as lateral and linear quadrupoles, can be constructed from arrays of elementary monopoles and dipoles. (Backman, 2005; Fahy, 2001; Hongisto, 2007)

The primary classification with regard to temporal characteristics involves determining whether the sound signal is stationary with regard to time or not. Further, the sound signal can be classified as either deterministic or random, and as transient or continuous. In the case of transient signals, it is more prudent to consider the acoustic energy released in the transient event, whereas continuous stationary signals are best analyzed with regard to their power characteristics. (Lahti, 1995)

The final categorization of sources is with regard to their spectral characteristics. As per Parseval's theorem, temporal and spectral signals display the same information in different forms, but it is useful to consider the spectral characteristics independent of their temporal duals. The source can be broadband or narrowband, contain discrete tones or random noise. This spectral analysis can and should consider the sensitivity of human hearing, and in most cases it is prudent to apply frequency weighting for the acquired spectra. The most typical weighting is A-weighting (see Figure 6), which can be seen as closely resembling an inverted equal-loudness contour at low loudness levels, as illustrated in Figure 5. This has the desired effect of attenuating the significance of weakly perceived auditory frequencies, and generally providing a high correspondence with the perceived loudness level (Lahti, 1995). The numerical values for A-weighting for one-third-octave bands

are given in IEC 61672 (2000).

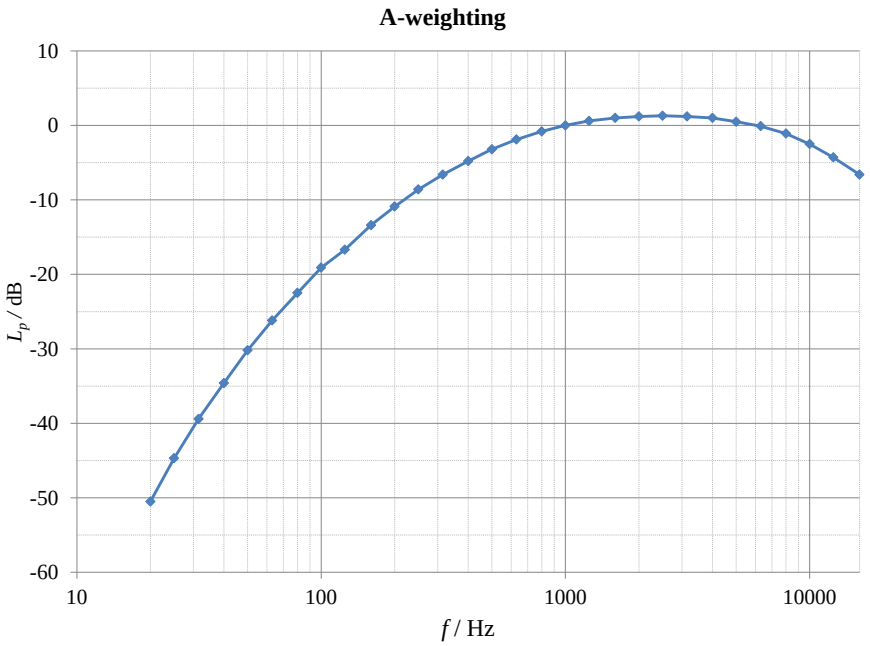

Figure 6: A-weighting of auditory frequencies (in one-third octave bands) as per IEC 61672 (2000).

3.3 Structural acoustics

The previous discussion of acoustic waves applies only to fluid media, and not to waveforms in solids. Solids, in this regard, differ from fluids primarily because solids can support shear stresses whereas fluids cannot (Cremer et al., 2005). The primary effect of this is that in practically all situations the only waveform present in fluids is the longitudinal wave, where displacement is parallel to wave propagation. In solids, however, significant energies can be transmitted by different waveforms. The field of study concerning sound generation and propagation in solids is called *structural acoustics*.

The most elementary cases are the pure longitudinal and pure transverse waves. In considering these cases, it is useful to consider examples where one or two of the considered dimensions are of trivial lengths; i.e. they can be approximated either as zero or as infinite. Henceforth they shall be named trivially dimensioned cases. Pure transverse and pure longitudinal waveforms can only exist in trivially dimensioned objects, as in non-trivially dimensioned objects a contraction in one dimension is countered by an expansion in the other dimensions and vice versa. Thus, actual longitudinal waves in non-trivially dimensioned systems are better referred to as *quasi-longitudinal waves*. (Cremer et al., 2005)

Transverse waves in solids can take one of three physically significant forms. The first is "regular" transverse motion, such as the vibration of a guitar string or drum membrane (both trivially dimensioned in most cases), where the displacement is normal to the plane surface. The second case is *in-plane transverse waves* where displacement happens in the plane of the vibrating surface, such as the above drum membrane. The third type is the *rotational wave*, where the displacement is angular rather than linear. (Cremer et al., 2005; Fahy, 2001)

The most important type of waveform in solids is the *bending* or *flexural wave*. This is a waveform in non-trivially dimensioned objects where an element of the vibrating body undergoes both rotational and translational displacements, as well as both compression and expansion. The unique property of bending waves is that the waveform is *dispersive*, i.e. the speed of wave propagation depends on its frequency – more specifically the square root of the frequency. This has the effect that wavelength is also dependent on frequency, and this in turn has significant implications for noise control. (Cremer et al., 2005; Fahy, 2001; Backman, 2005; Hongisto, 2007)

The fourth type of solid waveform is the *surface wave*, where the displacement is inversely proportional to the distance from the boundary, but this has little implications for small objects, as the wavelength of vibration must be small compared to the thickness of the object, thus limiting this waveform, in most cases, to ultrasound frequencies. (Cremer et al., 2005; Backman, 2005)

In practice, most acoustic energies are radiated by bending waves, but other waveforms, particularly longitudinal waves can transmit significant acoustic energies throughout mechanically coupled systems.

Thus, the process of structural sound presents itself as such seen in Figure 7. The source, or generator, is always a component that generates fluctuating forces at auditory frequencies. This vibration is then coupled, or transmitted, to adjacent surfaces. Then, the each subsequent surface also couples with all other connected surfaces in the propagation stage. Finally, the surface normal component of said mechanical vibration is radiated to the surrounding medium at boundaries. (Cremer et al., 2005)

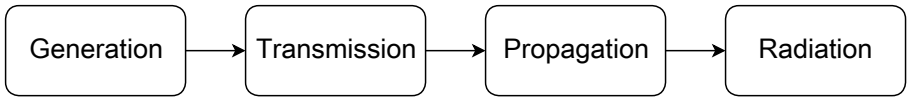

Figure 7: Generation process of structural sound. (Cremer et al., 2005)

The whole process of structural acoustics differs from airborne sound in that the original source of vibration need not be the radiator of sound. This leads us to inspect the vibrating system at a variety of levels: the component causing the vibration, the network of connected surfaces and the final radiation into the medium.

The intermediary stage of connected surfaces can essentially be understood as a system of connected mechanical impedances (Tanttari and Saarinen, 1995). Mechanical impedances are specific to the types of vibration (Fahy, 2001).

Each object has certain vibratory properties that are specific to the dimensions, form, material, frequency and waveform. Vibration in a body can be either *resonant* or *forced*. Forced vibration can occur at any frequency and any waveform. Resonant vibration, on the other hand, occurs only when the waveform occurring in the body "fits" the body so that incident and reflected waves amplify each other at boundaries. In a rectangular plate, for example, the lowest resonant frequency occurs when one of the dimensions is half the wavelength of a type of vibration. (Fahy, 2001)

An important case to notice here is the dispersive nature of bending waves. Because the speed of propagation of vibration increases with frequency, in most cases there exists a frequency for which the speed of sound in the solid, c_S, equals the speed of sound in the medium, c_0. When this is the case, both the frequency and wavelength are the same in both the medium. This frequency is termed the *frequency of coincidence*. At this frequency, coupling between the solid and the medium is strong, and conversely, insulation for airborne sound is weak. (Tanttari and Saarinen, 1995; Hongisto, 2007)

The propagation of sound through surfaces, both airborne and structural, depends on the resonant or *modal* characteristics of the surface. The most common type of surface in small machines is a plate structure. For plates, the vibrations at frequencies below the resonances are governed by the stiffness of the plate. At resonant frequencies, the vibration is restricted only by the damping of the structure. Above the first few resonant frequencies, it is the mass of the plate that determines its resistance to vibration. Typically, coincidence occurs in this region, or the so called *mass law* region. *Transmission loss* is the amount of damping (in decibels) a structure exhibits for the propagation of airborne sound. This behaviour is illustrated in Figure 8. (Tanttari and Saarinen, 1995)

Finally, the generation of structural sound is dependent on the *radiation efficiency* of the structure that is in contact with the surrounding medium. In essence, radiation efficiency is defined as the ratio of sound power to average mean square normal velocity of the surface. Radiation efficiency is high when the length of a uniformly vibrating surface is in the same order as the wavelength of vibration in air. (Fahy, 2001; Tanttari and Saarinen, 1995)

3.4 Sound generation in axial flow fans

Noise from axial flow fans has been touched in Section 3.2, but will be detailed more here. Axial flow fans primarily generate airborne noise via a Category 2 source.

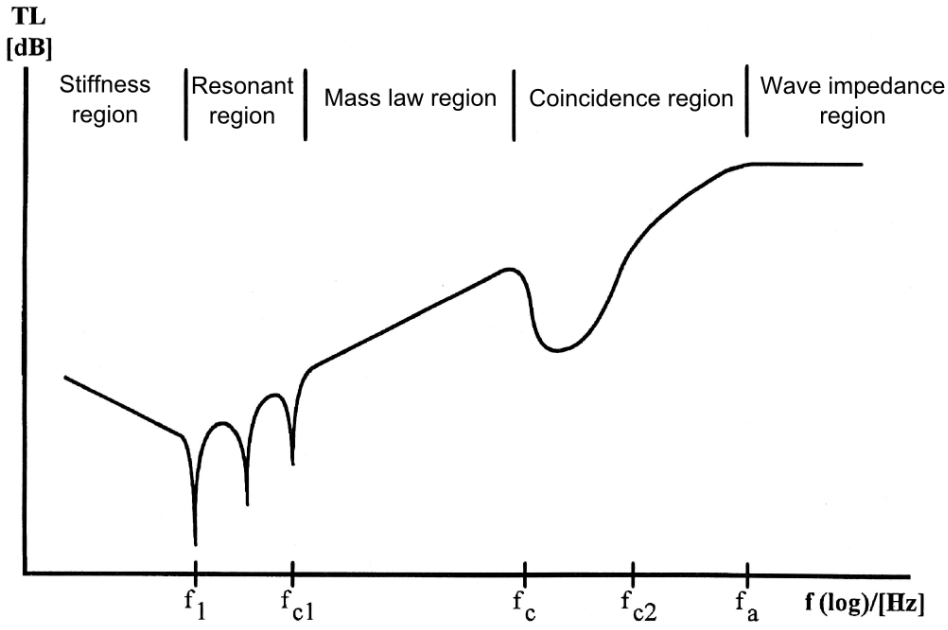

Figure 8: Transmission loss of a rigidly attached vibrating plate. TL = Transmission loss, or the amount by which the structure attenuates sound at a given frequency. (Tanttari and Saarinen, 1995)

Flow unsteadiness around the rotor blade causes alternating low pressure zones in the wake of the blade, causing vortex shedding. Since in most fans the blades are affixed to the rotor at uniform angular intervals, vortex shedding is periodic in time at the *blade passing frequency* (BPF), which is defined as the product of the angular frequency of rotation and the number of blades in the rotor. This is the main source of fan noise generation. (Gérard et al., 2005)

Besides the periodic fluctuations at BPF and its harmonics, fans also exhibit broadband noise. One of the main causative mechanisms of high frequency broadband noise is the presence of additional vortical flows at the *tip clearance*, or the distance from the outermost point of the rotor to the innermost point of the stator. Leakage of flow in this gap is related to acoustic noise emissions at frequencies far above BPF and its first few harmonics. According to Quinlan and Bent (1998), reducing tip gap in their experimental design caused reduction of up to 9 dB per octave band at frequencies above 2 kHz. (Quinlan and Bent, 1998; Maaloum et al., 2003) Fukano and Jang (2004) posit that spectral peaks at BPF and its first four harmonics are due to periodic velocity fluctuations, and the broadband noise is due to flow velocity unsteadiness.

Maaloum et al. (2003) provide a further breakdown of noise generation mechanisms in axial fans. Of the ones not discussed yet, the most significant source at low speeds (defined variously at either 0.7 or 0.8 Mach peripheral rotor speeds) is

turbulent inflow. Providing a more laminar airflow can provide benefits up to 10 dB at BPF. This can be achieved by contouring the inlet duct (Maaloum et al., 2003) or by modifying upstream obstacles such as the grid or fingerguard in the case of surface-mounted fans (Otto et al., 2006). Otto et al. (2006) present variations in broadband noise emissions of up to 2.1 dB by varying grid rib profiles, variations up to 6.5 dB by varying grid geometry and negligible changes in emissions by varying distance between grid and rotor.

3.5 Sound generation in chokes

Audible noise is a typical problem of iron core inductors such as chokes typically are (Thorborg, 1988), and as has been previously noted, almost all choke noise is due to a ferromagnetic phenomenon called *magnetostriction* (John J. Winders, 2002). Magnetostriction is a phenomenon, where the shape of a ferromagnetic object changes as a function of magnetization. This is due to the fact that in an demagnetized state the alignment of individual crystals is effectively random and becomes increasingly aligned parallel to magnetic field lines. This causes rotation of the crystals, and thus a deformation of the object's body and a change in its volume (Chikazumi, 1997). Magnetostriction is an essentially nonlinear phenomenon as crystal alignment approaches parallel, magnetostrictive strain becomes saturated.

Weiser et al. (2000) present a division of noise sources into core magnetization noise and winding noise. Magnetization noise is considered more important of the two. Both Krell et al. (2000) and Weiser et al. (2000) acknowledge transformer core noise resulting from both magnetostriction and magnetostatic forces. However, optimizing the design of a laminated steel transformer can yield significant decreases in noise of magnetostatic origin and allow us to predict core noise by magnetostriction alone (Weiser et al., 2000).

4 Acoustic research methods and equipment

Acoustic research is carried out in a variety of conditions, each with its own benefits and limitations. To accommodate this variation, there are a number of acoustic research methods and a bevy of different tools to make the most of each situation. Below is a brief overview of the most common equipment and standardized methods of acoustic research.

4.1 Acoustic research equipment

4.1.1 Microphones

A microphone is a pressure-sensitive electroacoustic transducer. Most measurement microphones are *condenser microphones*, as they are stable, spectrally flat on a large bandwidth, have large dynamic range, small internal noise and are moderately sensitive. A condenser microphone generates an electrical signal by varying the distance between a charged backplate and the diaphragm (see Figure 9), thus acting as a film capacitor. A condenser microphone has a very small capacitance, and requires significant impedance matching. Thus a preamplifier is almost always a part of the microphone assembly. A typical measurement microphone with the associated preamplifier can be seen in Figure 10. (Lahti, 1995; Brüel & Kjær, 1996)

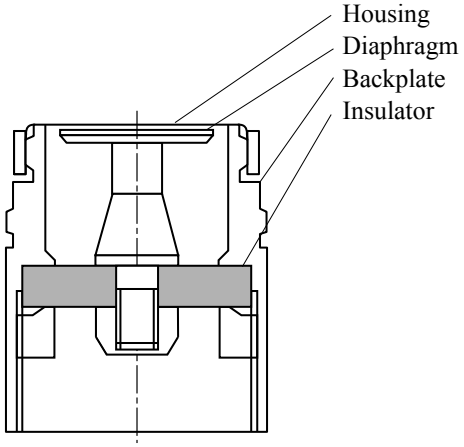

Figure 9: A cross section of a typical microphone capsule.

The main types of microphone are the *pressure microphone* and the *pressure gradient microphone*. The ideal pressure microphone is an enclosed space separated from the outside field with the diaphragm. The pressure differential then causes perturbations in the diaphragm's displacement along the axis of the microphone. The ideal pressure gradient microphone, on the other hand, exists only in the surrounding field. Therefore, the diaphragm is displaced only when there exists a pressure

Figure 10: B&K 4189 microphone with 2671 preamplifier.

gradient along the axis of the microphone. Most microphones are between the ideal extremes, and thus exhibit varying sensitivity in different directions. A microphone's upper usable frequency limit is determined by the mechanical resonances of the diaphragm and the reflections of the microphone capsule. (Lahti, 1995; Backman, 2008) Performance standards of measurement microphones are presented in IEC 61094 (2000).

4.1.2 Sound intensity probes

The determination of sound intensity requires information of particle velocity. However, there are no viable methods of measuring particle velocity directly. On the other hand, Equation 1 (on Page 7) gives us particle velocity as a function of the pressure gradient. We can approximate the pressure gradient by placing two pressure microphones in close proximity to each other at a fixed distance on the same axis (see Figure 11). This array is known as a *sound intensity probe*. Expressed in frequency domain, particle velocity is approximated as

$$U(f) = \frac{1}{j\omega\rho d}[P_1(f) - P_2(f)], \tag{8}$$

where U and P represent the Fourier transforms of particle velocity and sound pressure, respectively, f is the frequency of the sound, and d is the spacing between the microphones (Figure 11). Sound pressure is approximated as the mean sound pressure between the microphones as

$$P(f) = \frac{1}{2}[P_1(f) + P_2(f)]. \tag{9}$$

Taking a cross spectrum of these yields eventually

$$I(f) = -\frac{1}{\omega\rho d}\mathfrak{Im}\{G_{12}(f)\}, \tag{10}$$

where I is the Fourier transform of sound intensity, ω is angular frequency, and G_{12} is the cross spectrum of the microphones' pressure spectra. Thus, this assembly allows us to measure sound intensity propagating along the axis connecting the

two microphones. (Lahti, 1995) Performance standards for sound intensity probes are given in IEC 61043 (1993). A typical sound intensity probe is illustrated in Figure 4.1.2.

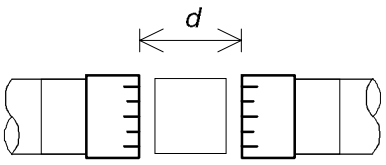

Figure 11: Placement of pressure microphones at separation distance d.

Figure 12: B&K 3595 sound intensity probe.

4.1.3 Sound calibrators

A *sound calibrator* is an electroacoustic device that generates a known sound field at a known position. The electrical signal given by a microphone can then be measured and the sensitivity of the microphone thus calibrated. Definitions and performance standards are given in IEC 60942 (2003). A sound calibrator is illustrated in Figure 13.

Figure 13: B&K 4231 sound calibrator. Microphone capsule is placed in the central opening for calibration.

4.1.4 Sound level meters

A sound level meter is an assembly that consists of a microphone, its preamplifier, a filter set, and a detector (Lahti, 1995). The filters are typically weighting filters and/or octave or fractional-octave filters (specified in IEC 61260 (1995)). The detector circuit performs RMS averaging and time integrating to yield readable values (Figure 14). The time integration uses exponential decay with either a 125 ms (fast) or 1000 ms (slow) time constant. Performance standards of sound level meters are specified in IEC 61672 (2000). A hand-held sound level meter is illustrated in Figure 15.

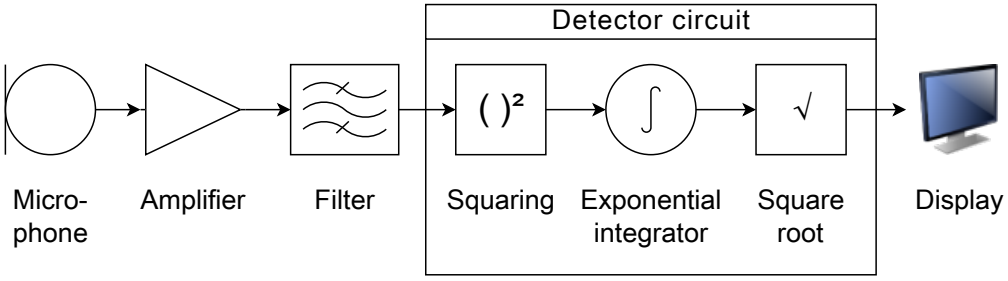

Figure 14: Block diagram of an averaging sound level meter.

Figure 15: B&K 2250 sound level meter with microphone windscreen.

4.1.5 Reference sound sources

A *reference sound source* (RSS) is a device that produces a sound emission at a known sound power level. Thus, we can compare the empirically determined sound power level against the known sound power level, and make appropriate adjustments in the interpretation of measured data. Specifications for the performance standards of reference sound sources are given in ISO 6926 (2000). A typical RSS is illustrated in Figure 16.

Figure 16: B&K 4204 reference sound source.

4.2 Measurement standards

There are a number of ISO standards relevant to the exploration of sound emissions of devices. These standards can be coarsely grouped into the following categories:

1. Standards specifying methods for the determination of sound power for use in various circumstances
   (a) Methods based on the measurement of sound pressure (ISO 3740 series)
   (b) Methods based on the measurement of sound intensity (ISO 9614)
2. Standards specifying methods for the determination of sound pressure levels at discrete points (ISO 11200 series)
3. Standards defining the presentation format of noise emission values (e.g. ISO 4871)
4. Standards defining a standard sequence of measurements for a class of devices (a noise test code; various ISO and IEC standards)
5. Standards defining the process to develop an aforementioned noise test code (ISO 12001)
6. Standards specifying performance requirements for equipment and facilities pertaining to the measurement of sound (various ISO and IEC standards)

These standards are prepared by ISO Technical Committee (TC) 43 (Acoustics) and its subcommittees, and by IEC TC 29 (Electroacoustics). Neither of these organizations had produced noise test codes for frequency converters or solar inverters at the time of measurement (May–July 2012). The most similar group of devices that had noise test codes specified was the rather broadly defined "information technology and telecommunications equipment" in ISO 7779, and "computer and business equipment" in ISO 9295 and ISO 9296. A peculiarity for these groups of devices,

which proved to be relevant, is that these families of devices commonly exhibit significant audible noise above 10 kHz, mainly due to small axial fans. In the general case, the A-weighted single-number sound emission level to be presented is limited to the frequency band of 100 Hz – 10 kHz. However, ISO 9295 presents methods for the determination of high-frequency noise, and ISO 9296 specifies the presentation of such results.

4.2.1 Standards for the determination of sound power

ISO 3740 (2000) is an overview standard that covers the various methods presented in ISO 3740 series standards and ISO 9614, and presents the criteria to consider when choosing the most appropriate standard. These criteria are:

1. Accuracy grade
2. Size and transportability of machinery and equipment
3. Available test environment
4. Background noise level
5. Acoustical instrumentation available
6. Acoustic characteristics of source and the information to be extracted (spatial, temporal and spectral)

The grades of accuracy are specified in ISO 12001 (1996), and are:

- *Survey grade* (Grade 3), which is used mostly to compare devices of similar acoustic characteristics *in situ*, with little control of the acoustic environment. Class 2 instrumentation is sufficient for this grade. No spectral information is extracted.
- *Engineering grade* (Grade 2), which is intended for use in noise emission declaration purposes. Instrumentation is expected to conform to Class 1 requirements, and the requirements imposed upon the acoustic environment are more stringent. Acoustic information may be presented in octave or one-third-octave frequency bands.
- *Precision grade* (Grade 1), which is intended for use where maximum accuracy is required. Instrumentation is the same as for Grade 2, but the requirements on the environment become even more stringent — true anechoic, hemi-anechoic or reverberation rooms are required. Recording of temporal and spectral information becomes mandatory.

In selecting the appropriate methods, most latitude with regard to environmental requirements is given to measurements based on sound intensity, i.e. ISO 9614. For survey methods, difference between source and background noise levels, ΔL, must be over 3 dB; for engineering methods, $\Delta L \geq 6$ dB (4 dB for reverberation rooms); and $\Delta L \geq 10$ dB for precision methods. Environmental trueness, i.e. the difference between theoretical and measured sound pressures at the measurement surfaces, must be less than 7 dB for ISO 3746 and less than 3 dB for ISO 3744.

Of methods based on sound pressure, ISO 3741 (Grade 1) and ISO 3743 (Grade 2) use hard-walled or reverberation rooms; ISO 3744 (Grade 2) utilizes an essentially hemi-anechoic space, ISO 3745 (Grade 1) requires anechoic or hemi-anechoic test chambers, and ISO 3746 and ISO 3747 (both Grade 3) specify no special restrictions on the test environment.

With regard to instrumentation, there is a conflict between ISO 3740 and ISO 12001: ISO 12001 states that Grade 3 methods can use Class 2 measurement equipment, whereas ISO 3740 gives this latitude only to methods based on sound intensity. However, the text body of ISO 3746 permits usage of Class 2 equipment, although Class 1 is recommended. The text body of ISO 3747 states that Class 1 equipment must be used. Thus, it can be concluded that ISO 3740 is unclear with regard to ISO 3746, and should be clarified. Only ISO 3744 and ISO 3745 allow us to obtain measurements of directivity information of the source.

4.2.2 Standards for the determination of emission sound pressure levels

As ISO 3740 advises on the selection of the appropriate standard for the determination of sound power levels, ISO 11200 serves in this function in the determination of emission sound pressure levels at specified positions. As with ISO 3740 series standards, ISO 11200 series standards differ with regard to accuracy grade and available equipment and facilities. Accuracy grades are identical to those in the ISO 3740 series. However, no standard in the ISO 11200 series conforms to the requirements of Grade 1 accuracy.

The three primary categories of ISO 11200 series standards are

- Methods based on direct measurement of sound pressure (ISO 11201, ISO 11202, ISO 11204)
- Method based on measurement of sound intensity (ISO 11205)
- Method based on calculation from measured sound power levels (ISO 11203)

Of the first category, the primary differences are between required environmental corrections. ISO 11201 is intended for laboratory use, while ISO 11202 and ISO

11204 are *in situ* methods. ISO 11202 is a survey method, while ISO 11204 allows for greater accuracy.

The second category – or simply ISO 11205 – is an engineering method (Grade 2) intended for use *in situ* as an alternative to the standards in the previous category.

The third category provides us accuracy grades conforming to those of the standards used to obtain sound power levels. ISO 11203 is most applicable for devices which need not be continuously operated and are relatively small in dimension.

4.2.3 Standards on noise test codes

As defined by ISO 12001, a noise test code is

> *"A standard that is applicable to a particular class, family or type of machinery or equipment, which specifies all the information necessary to carry out efficiently the determination, declaration and verification of the noise emission characteristics under standardized conditions."*

The requirements of a noise test code, as specified by ISO 12001, are that a noise test code must specify:

- Accuracy grade to be utilized — Grade 2 is preferred unless compelling reason is given to allow Grade 3
- Measurement standard(s) to be utilized in determining sound power emission levels
- Measurement standard(s) to be utilized in determining emission sound pressure levels at workstations and/or specified positions
- Method for declaring acquired results
- An accurate description of the family or class of devices
- All ancillary equipment and sub-assemblies necessary for the operation of the devices
- Operating procedures for cases where the device cannot be uncoupled from surrounding devices and tested independently
- The process for determining A-weighted sound power levels and emission sound pressure levels
- Installation and mounting conditions of the devices

- Operating conditions for the devices or machinery
- Measurement uncertainties
- Information to be reported when following test code in question

Although ISO TC 43 Subcommittee 1 (Noise) has not produced any specified noise test code for this family of devices, it has produced ISO 7779, which is intended for "information technology and telecommunications equipment", i.e. standard office paraphernalia such as printers, projectors and keyboards (specific reference is given to ECMA-74, where these equipment classes are defined). Thus, while these categories are not directly applicable to solar inverters, significant conformity exists with regard to installation and operation conditions and spectral characteristics of some of these device classes.

In short, wall-mounted devices (solar inverters frequently are) shall be mounted either to the wall of a reverberation room or with the mounting surface laid on the floor of a hemi-anechoic chamber. All walls shall be at least 1.5 m, and preferably 2 m, from the device.

The devices shall be operated at their nominal rated voltage and rated power line frequency, up to a tolerance of 5%. The device shall be oriented "in a manner typical of normal use". If multiple operating modes are defined, the most common mode shall be tested and reported. Also, the device shall be tested in its idle mode.

ISO 7779 allows sound power determination to occur either in accordance to ISO 3741 or to ISO 3744, and the environment and equipment shall conform to the requirements specified within the aforementioned standards. Workstation emission sound pressure levels shall be measured in accordance to ISO 11201.

The test report shall provide sufficient description of all involved equipment and their operational characteristics. All acoustic emission information is to be reported rounded to the nearest 0.1 dB. Information shall be recorded in octave-bands with center frequencies from 125 Hz to 8 kHz and presented as a broad-band A-weighted figure. Whether high-frequency noise exists (i.e. in the 16 kHz octave band), it shall be reported in accordance with ISO 9295.

ISO 9295 specifies a number of methods for the determination of high-frequency noise, one of which essentially conforms with ISO 3744. However, with regard to reporting of high-frequency noise, there exists a conflict between ISO 7779 and ISO 9295. ISO 9295 allows the extension of the upper bound of the A-weighted noise emission frequency band from 10 kHz to 20 kHz in cases where the high-frequency noise is broad-band in character. However, the more recently updated ISO 7779 allows only the reporting of unweighted one-third-octave frequency band levels in addition to the A-weighted sound power level in cases where the noise is broad-band

in character. In cases where the noise emission in the 16 kHz octave band is tonal in character, unweighted narrow-band sound power levels and their frequencies must be reported separately for each tone that is within 10 dB of the most significant tone.

4.2.4 Standards concerning the presentation of noise levels

After relevant measurements and calculations have been carried out, the information needs to be presented in a form that makes these figures comparable across a range of devices. For this purpose, the normative reference given in ISO 3740 and ISO 11200 series standards is to ISO 4871.

According to ISO 4871, all noise emission declarations shall contain the following information:

1. Identification of the machinery or equipment
2. Identification of the noise test code and/or basic standards used to obtain the declared values
3. Identification of the respective operating modes
4. Either
   (a) the words "DECLARED SINGLE-NUMBER NOISE EMISSION VALUES in accordance with ISO 4871" followed by one or more single-number noise emission values L_{WAd}, L_{pAd} or $L_{pC,peak,d}$
   (b) the words "DECLARED DUAL-NUMBER NOISE EMISSION VALUES in accordance with ISO 4871" followed by one or more single-number noise emission values L_{WAd}, L_{pAd} or $L_{pC,peak,d}$ and their associated uncertainties K_{WA}, K_{pA} or $K_{pC,peak}$

ISO 4871 further specifies that the preferred noise emission quantity to be declared is L_{WA} in either single- or dual-number version. Special note is given that for computer and business equipment, for which ISO 7779 applies, the declaration of noise emission values should follow instead ISO 9296.

When declaring single-number noise emission values, the associated measurement uncertainty is to be included within the value according to the expression

$$L_d = L + K, \tag{11}$$

where L is the noise emission quantity and K is its associated uncertainty.

The primary differences between ISO 4871 and ISO 9296 are that ISO 9296 mandates that noise emission tests be carried out on a representative batch of equipment, that all declarations be single-number values, that declarations be made both of sound power and emission sound pressure levels, and, for some reason, that declarations be made in bels instead of decibels.

5 Presenting the test case

5.1 Devices to be tested

The first goal of this thesis is to investigate the sound power emissions of a number of on-market devices. To accomplish this goal, the following devices were selected:

Table 1: Devices to be investigated

Device name	Rated max. power	Declared noise emission
Danfoss TLX 15	15 kW	max. 56 dB(A)
Fronius IG TL 5.0	5 kW	N/A
Kostal PIKO 8.3	8.3 kW	33...46 dB(A)
PowerOne Aurora Trio 20.0	20 kW	$<$ 50 dB(A) @ 1 m
PowerOne PVI-3.0	3 kW	$<$ 50 dB(A) @ 1 m
REFUsol 017K	16.5 kW	$<$ 45 dBA
SMA Sunny Tripower 6000TL	6 kW	40 dB(A) (typical)
Voltwerk VS 15	15 kW	N/A

As can be seen, none of the above devices conform to either ISO 4871 or ISO 9296 with regard to the declaration of noise emission. Three out of eight manufacturers did not even report a noise emission value. When a noise emission was reported, no indication as to how these figures were obtained was given.

5.2 Choice of method

It was determined that ISO 7779, along with its companion standards ISO 9295 and ISO 9296, would serve as the basis of the measurement plan. The facilities and equipment would allow for Grade 2 accuracy, so that was chosen as the desired accuracy grade. Sound power was to be determined via ISO 3744, with a 10-microphone hemispherical measurement surface.

The first significant deviation from ISO 7779 comes in the determination of emission sound pressure levels. While ISO 7779 demands ISO 11201 to be used to obtain emission sound pressure levels, this method was forgone in favor of calculating them via the methods specified in ISO 11203. The main reason for this was that due to the large batch of machines and operating points to be tested, it would speed up the measurement process significantly if the microphone assembly need not be modified often. After-the-fact estimation from previously obtained data, on the other hand, could be easily replicated. The second major deviation from ISO 7779 is that contrary to the requirements of the standard, multiple operating modes were chosen for each device.

The third deviation from ISO 7779 is in the presentation of high-frequency noise. First, the equipment available precluded measurements for the 20 kHz one-third-octave band, only extending the range up to the 16 kHz one-third-octave band. Second, the conflict between the presentation of high frequency noise in ISO 7779 and ISO 9295 lead to the presentation two complementary methods were presented in addition to the standard L_{WA}. Thus, it was deemed sensible that three sound power figures should be presented:

1. $L_{W,A}$, or broadband A-weighted sound power level containing the frequencies between 100 Hz and 10 kHz
2. $L_{W,A,16k}$, or A-weighted sound power level for the 16 kHz octave band (sans the 20 kHz one-third-octave band)
3. $L_{W,A,ext}$, or broadband A-weighted sound power level containing the frequencies between 100 Hz and 20 kHz

Case 2 was chosen to be A-weighted rather than unweighted (as per ISO 7779), since the purpose of the evaluation of noise emission is the subjectively perceived loudness rather than physically existing energy levels.

5.2.1 Determining sound power levels via ISO 3744

In order to procure quantitative measures via ISO 3744, there exist a number of checks for the adequacy of the testing procedure:

- Determine adequacy with regard to background noise levels (relative and absolute)
- Determine environmental correction
- Calibrate instruments (pre and post)

The relative adequacy with regard to background noise is that the level of sound pressure on a one-third-octave band shall exceed the level of the background noise by a minimum of 6 dB and preferably by 15 dB. Failing that test, if the one-third-octave level of background noise is at or below the absolute criterion, as illustrated in Figure 17, conformity with the requirements of ISO 3744 can be said to have been met. If any fractional-octave bands fail the noise clearance criterion, they shall be excluded from the calculation of A-weighted levels. If the difference between the A-weighted levels before and after the exclusion of the nonconforming bands exceeds 0.5 dB, the entire A-weighted level shall be considered invalid.

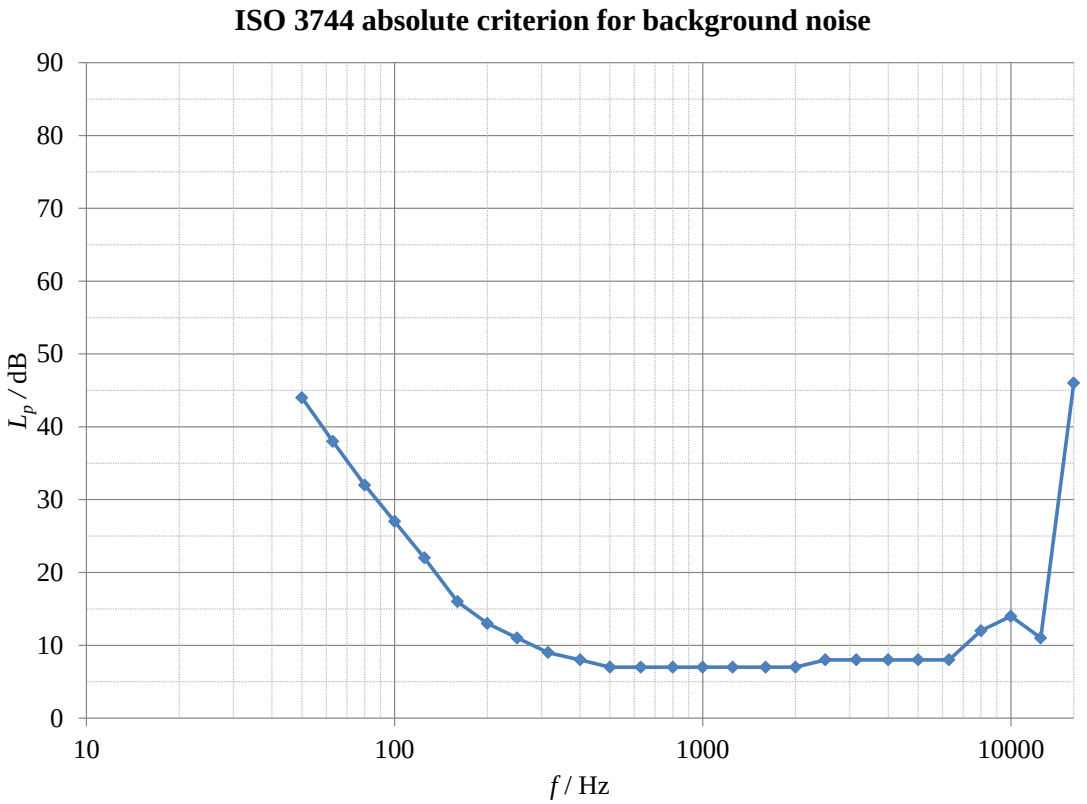

Figure 17: ISO 3744 absolute criterion for background noise.

The environmental correction for the measurement space was determined by the absolute comparison method specified in Annex A of ISO 3744. According to this process, a reference sound source conforming with ISO 6926 (2000) is placed in essentially the same place as the device(s) under test. Then, when the environmentally uncorrected sound power measurements (detailed below) are obtained, they are compared against the known sound power emission of the reference sound source, and the environmental correction term K_2 is obtained by the equation

$$K_2 = L_W^* - L_{W(\mathrm{RSS})}, \tag{12}$$

where L_W^* is the environmentally uncorrected measured sound power, and $L_{W(RSS)}$ is the sound power level of the calibrated reference sound source.

To ascertain the validity of the measurements, ISO 3744 states that microphones must be calibrated before *and* after the measurements. If the difference between the sensitivity levels of the microphones before and after measurements is more than 0.5 dB, the measurements should be discarded. It is important to note, that due to time and facility constraints, a post-measurement calibration process was not undertaken, and thus *none of the results in this thesis can be said to conform*

with ISO 3744.

ISO 3744 is based on the assumption, that, given adequacy of the test environment, all sound emanating from the source is distributed on a *measurement surface*, on which all measurement points are essentially equidistant from the noise source. The choice of measurement surface is determined by the relation between the size of the source and the size of the environment, i.e. whether the measurement points are considered to be in the acoustic near-field or not. To determine this, ISO 3744 specifies that a rectangular parallelepiped surface enclosing the furthest protrusion of the acoustic source, called the *reference box*, shall be determined. Then, the characteristic dimension d_O is determined as the distance from the acoustic center of the reference box to the corner of the box, as illustrated in Figure 18, and given by the equation

$$d_O = \sqrt{(\frac{l_1}{2})^2 + (\frac{l_2}{2})^2 + l_3^2}, \tag{13}$$

where l_1, l_2 and l_3 correspond to the dimensions of the device.

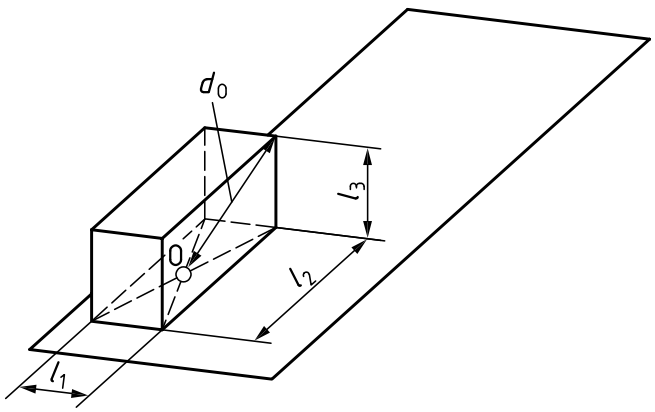

Figure 18: Reference box for device mounted on one reflective surface in a hemianechoic chamber. (ISO 3744, 2010)

It is assumed that measurements are taken in the acoustic far-field if it is possible to attain measurement distances (from the acoustic center of origin) that are at least twice the characteristic dimension of the source. If the assumption is satisfied, a hemispherical measurement surface such as illustrated in Figure 19 is suggested (although not required). Otherwise, a parallelepiped surface is suggested. In the parallelepiped surface, the measurement surface is taken as the reference box extended by the measurement distance d in each direction, as illustrated in Figure 20. Microphones are oriented normal to the measurement surface, except for the corner measurement positions, that are oriented towards the acoustic center of the

device. ISO 3744 also allows for cylindrical and combination surfaces, but these were not considered, given the small size of the devices.

Overall, the selection of a hemispherical measurement surface was deemed more appropriate, since the facilities could accommodate this choice, and given an appropriate measurement radius, the assembly need not be modified when the device is changed, as would have been the case if a parallelepiped surface would have been chosen.

To determine an appropriate measurement radius r, the characteristic dimension d_O for the batch of devices was determined. The dimensions of the devices according to Figure 18, as well as the characteristic dimension d_O as per Equation 13, are listed in Table 2.

Table 2: Dimensions of the devices under test

Device name	l_1	l_2	l_3	d_O
Danfoss TLX 15	0.525	0.700	0.250	0.504
Fronius IG TL 5.0	0.413	0.597	0.195	0.412
Kostal PIKO 8.3	0.450	0.520	0.230	0.414
PowerOne Aurora Trio 20.0	0.702	1.061	0.292	0.700
PowerOne PVI-3.0	0.325	0.618	0.222	0.414
REFUsol 017K	0.535	0.601	0.277	0.488
SMA Sunny Tripower 6000TL	0.470	0.730	0.240	0.496
Voltwerk VS 15	0.510	0.790	0.245	0.530
Generic Device*	—	—	—	0.651

* The exact dimensions of the Generic Device withheld at the behest of ABB

Thus, it is evident that a measurement radius r of 1.5 m is adequate for all devices, and hence was chosen for this thesis. The advantage of having the measurement radius as close to the $2d_O$ criterion as possible is that this maximizes the signal-to-noise ratio (SNR).

Once the measurement set-up was set, the acquisition of results proceeded as follows. First, time-averaged sound pressure levels $L'_{pi(ST)}$ from the source under test were obtained by measurement in frequency bands and as narrowband spectra. The measurement time was 20 s. After this, the mean time-averaged sound pressure level was determined according to the equation

$$\overline{L'_{p(\mathrm{ST})}} = 10\,lg\left[\frac{1}{N_\mathrm{M}}\sum_{i=1}^{N_\mathrm{M}} 10^{0.1L'_{pi(\mathrm{ST})}}\right], \tag{14}$$

where i is the microphone number and N_M is the number of microphones. If the microphone positions had been distributed unevenly in the space, each position's

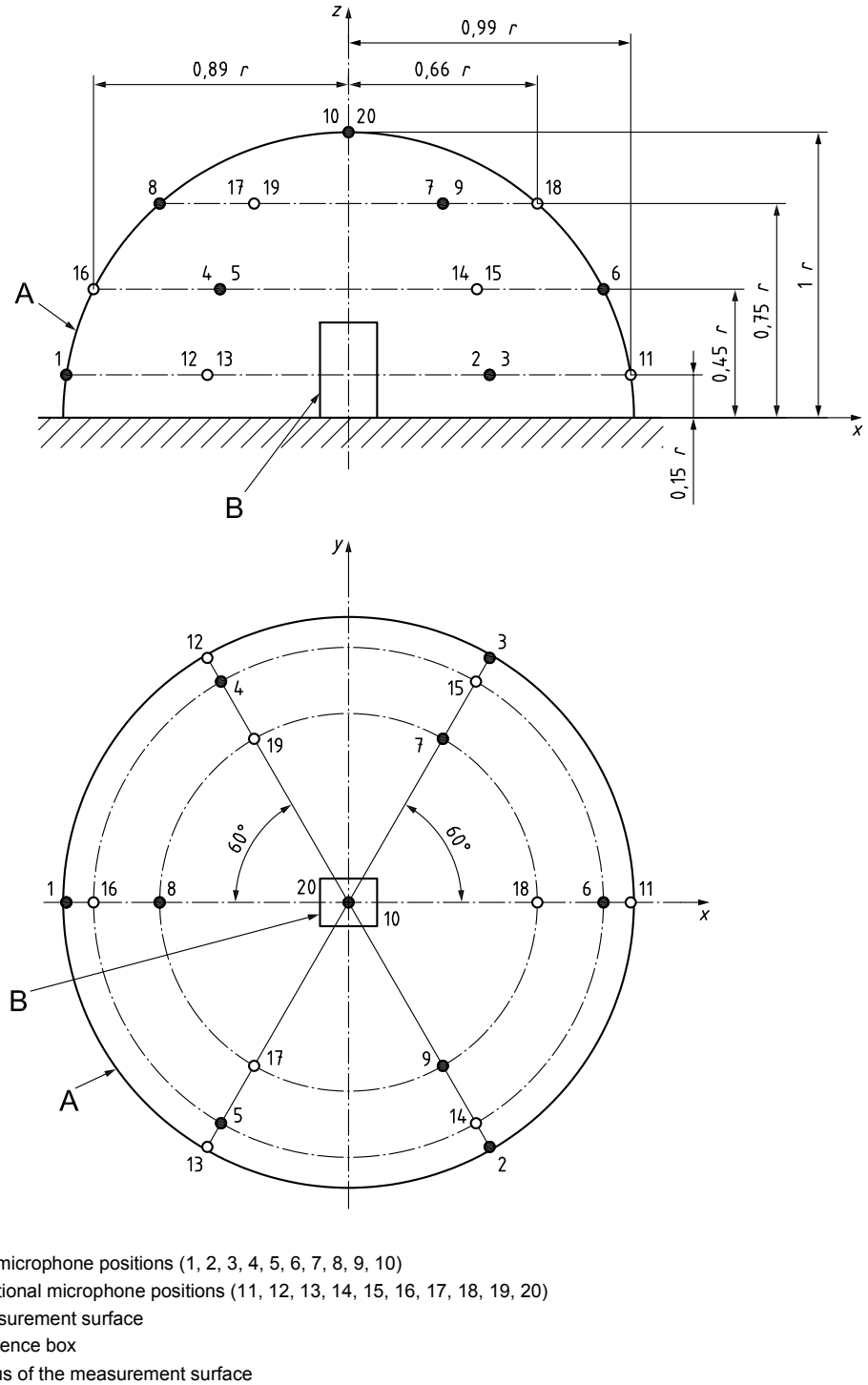

Key

- ● key microphone positions (1, 2, 3, 4, 5, 6, 7, 8, 9, 10)
- ○ additional microphone positions (11, 12, 13, 14, 15, 16, 17, 18, 19, 20)
- A measurement surface
- B reference box
- *r* radius of the measurement surface

Figure 19: Diagram of a hemispherical measurement surface. (ISO 3744, 2010)

level would have been weighted by the surface area it covers and averaged across total measurement surface area.

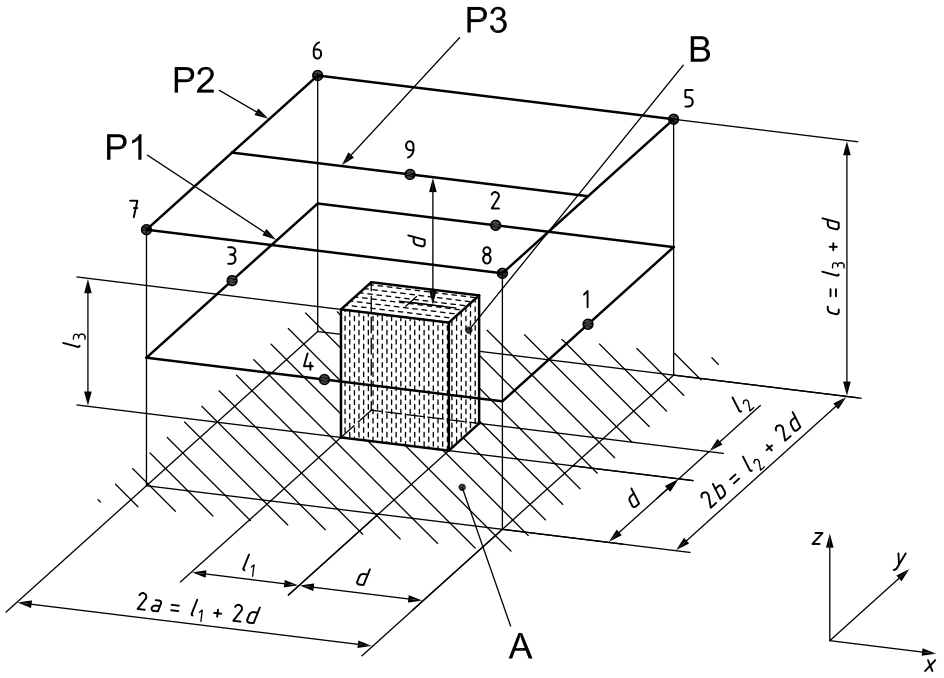

Key

●	key microphone positions
A	reflecting plane
B	reference box
$2a$	measurement surface length
$2b$	measurement surface width
c	measurement surface height
d	measurement distance
l_1	reference box length
l_2	reference box width
l_3	reference box height
P1 to P3	path 1 to path 3

Figure 20: Diagram of a parallelepiped measurement surface for a small device. (ISO 3744, 2010)

Similarly, mean time-averaged background noise level is acquired according to the equation

$$\overline{L'_{p(\mathrm{B})}} = 10\,lg\left[\frac{1}{N_{\mathrm{M}}}\sum_{i=1}^{N_{\mathrm{M}}} 10^{0.1L'_{pi(\mathrm{B})}}\right]. \tag{15}$$

When mean time-averaged sound pressure levels have been determined for both the source under test and the background noise, the background noise correction term K_1 can be determined by the equation

$$K_1 = -10\,lg\left(1 - 10^{-0.1\Delta L_p}\right), \tag{16}$$

where

$$\Delta L_p = \overline{L'_{p(\mathrm{ST})}} - \overline{L'_{p(\mathrm{B})}}. \tag{17}$$

If $\Delta L_p \geq 15$ dB, K_1 is assumed to be 0. If 6 dB $\leq \Delta L_p < 15$ dB, K_1 is determined according to Equation 16. If $\Delta L_p < 6$ dB, K_1 is assumed to be 1.3 dB. Additionally, if the band(s) where $\Delta L_p < 6$ dB do not meet the absolute criterion for background noise measurements, it shall be clearly stated that noise emission levels in those bands represent upper bounds, and that these figures are not in accordance to ISO 3744.

Once the correction terms K_1 and K_2 have been determined, the surface time-averaged sound pressure levels are determined according to the equation

$$\overline{L_p} = \overline{L'_{p\mathrm{ST})}} - K_1 - K_2. \tag{18}$$

Sound power levels, then, can be determined by the equation

$$L_W = \overline{L_p} + 10\,lg\frac{S}{S_0}\mathrm{dB}, \tag{19}$$

where S is the measurement surface and S_0 is 1 m^2. For a hemispherical measurement surface,

$$S = 2\pi r^2, \tag{20}$$

where r is the measurement radius.

In addition to the determination of sound power levels, ISO 3744 allows for the determination of apparent directivity indices D^*_{Ii} and apparent surface sound pressure level non-uniformity index V^*_I. D^*_{Ii} specifies how much sound is radiated in the direction of the ith microphone relative to the surface average, and is determined by the equation

$$D^*_{Ii} = L_{pi\mathrm{ST}} - \left[L'_{p(\mathrm{ST})} - K_1\right]. \tag{21}$$

V^*_I specifies how much, on average, the sound emission varies across all microphone positions. When measured at a radius r, it is to be denoted as V^*_{Ir}. For a measurement radius of 1.5 m, it is defined as

$$V^*_{I1.5} = \sqrt{\frac{1}{N_\mathrm{M} - 1} \sum_{i=1}^{N_\mathrm{M}} \left[L_{pi(\mathrm{ST})} - L_{p\mathrm{av}} \right]^2}, \tag{22}$$

where $L_{p\mathrm{av}}$ is the arithmetic mean of the background noise corrected sound pressure levels across all microphone positions.

The measurement uncertainty of ISO 3744 $u(L_W)$ is determined by the total standard deviation

$$u(L_W) \approx \sigma_\mathrm{tot}. \tag{23}$$

The total standard deviation is expressed as the RMS average of all constituent standard deviations of uncertainties. In this case, the most significant uncertainties are the standard deviation of the reproducibility of the method σ_{R0}, and the standard deviation of the instability of the mounting conditions σ_omc. Thus, the equation for total standard deviation becomes

$$\sigma_\mathrm{tot} = \sqrt{\sigma^2_{R0} + \sigma^2_\mathrm{omc}}. \tag{24}$$

Thus, the measurement uncertainty can be estimated from σ_tot by the equation

$$U = k\sigma_\mathrm{tot}, \tag{25}$$

where k is the coverage factor. For a normal distribution, a coverage factor of 2 corresponds to a 95 % confidence that the true value lies between $(L_W - U)$ and $(L_W + U)$.

σ_omc is chosen according to the task, and in the case where the time-variability of noise emission is small, and the measurement procedure is well defined, ISO 3744 states that a value of 0.5 dB for σ_omc can be appropriate. It was chosen to use this value in lieu of determining the value experimentally.

σ_{R0} is determined experimentally, but ISO 3744 provides typical upper-bound values in tabular form. ISO 9295 provides a corresponding value for high-frequency noise. The upper-bound values, along with total standard deviations and the corresponding uncertainties are presented in Table 3.

5.2.2 Determining sound pressure levels via ISO 11203

ISO 11203 is a standard that uses either a calculated or experimentally measured quantity Q to arrive from sound power levels to emission sound pressure levels.

Table 3: Standard deviations of reproducibility and measurement uncertainties in accordance with ISO 3744 and ISO 9295 (values in dB).

One-third octave band center frequency	σ_{R0}	σ_{omc}	σ_{tot}	U
100 to 160	3.0	0.5	3.0	6.1
200 to 300	2.0	0.5	2.1	4.1
400 to 5000	1.5	0.5	1.6	3.2
6,300 to 10,000	2.5	0.5	2.5	5.1
12,500 to 20,000	3.0	0.5	3.0	6.1
A-weighted	1.5	0.5	1.6	3.2

Because it is inherently linked to the standard by which sound power figures were determined, the time averages, frequency weightings and measurement uncertainties equal those procured in the determination of sound power levels. This method assumes sound propagation as in an essentially free field over a reflecting plane.

The experimental determination of Q is only applicable for cases where a noise test code provides experimentally determined values for Q.

Because no specified operator position exists for frequency converters or solar inverters, ISO 11203 is applicable if "an average sound pressure level over a measurement surface at a fixed distance ... from the reference box can be assumed to be representative".

The equation for determining emission sound pressure levels from sound power levels is as follows:

$$L_p = L_W - Q, \tag{26}$$

where

$$Q = 10lg\,\frac{S}{S_0}dB, \tag{27}$$

where S is a parallelepiped surface at distance d from the reference box (similar to the measurement surface in Figure 20 on Page 33), and S_0 is 1 m^2. According to ISO 11203, typical values for d are in the range of 0.3 m – 1.0 m. For the purposes of this thesis, d was taken to be 0.45 m; determined *ad hoc* as the approximate distance between the front panel of the devices and the middle of the line connecting the operator's ears when the device is operated at an arm's distance.

5.3 Testing facilities and equipment assembly

The acoustic measurements were carried out in a hemi-anechoic chamber at ABB's Helsinki campus. The acoustic environment meets the requirements of ISO 3744 (2010) on the frequency band from 100 Hz to 20 kHz. The space was measured against a Brüel & Kjær 4205 reference sound power source with B&K HP 1001 sound source. The sound source was also used to determine the environmental correction factors required by ISO 3744 (2010). The reference sound source was itself calibrated with a B&K 2250 sound level meter according to the device instructions. The sound level calibrator, in turn, was calibrated with a B&K 4231 microphone calibrator.

The device under test (DUT) was placed in the acoustic center of the test room. It was fed DC current from a Magna-Power current source. The AC current generated by the inverter was fed to a power resistor. The microphone assembly was a 10-point hemisphere according to ISO 3744 (2010). The radius of the microphone assembly was 1.5 m. This assembly has the property that each measurement latitude has microphones spaced 120° apart (Figure 19 on Page 32). The device was oriented so that the input cables faced the door and microphone 1, and measured four times, so that the orientation was changed 30° counterclockwise. In doing this, and assuming the noise sources to be stationary with regard to time, the measurement yielded microphones effectively spaced 30° apart on each latitude. Figures 21 and 22 detail the assembly at 0 and 60° rotation, respectively.

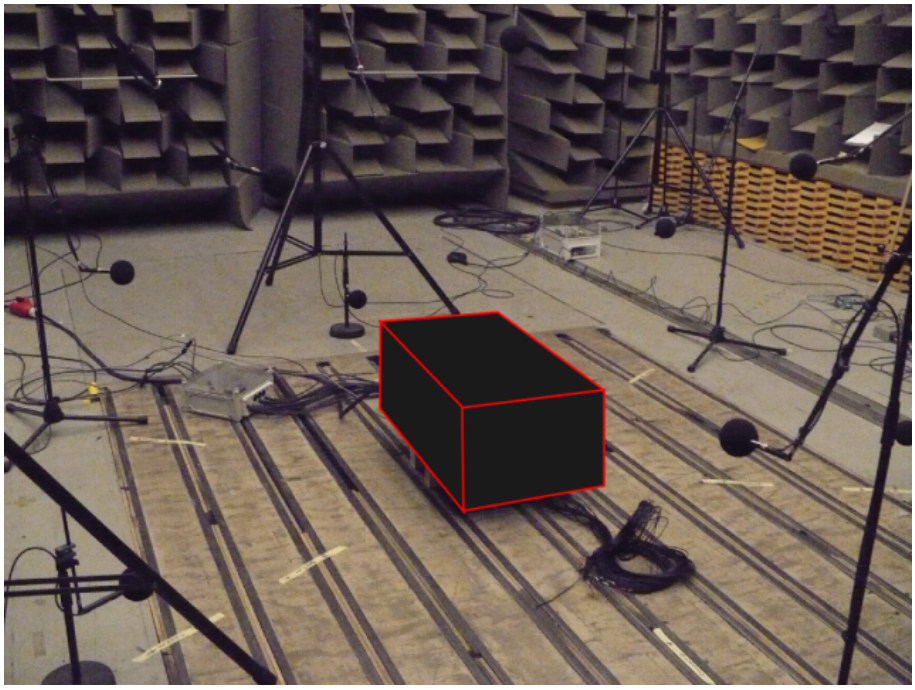

Figure 21: The test assembly at 0° rotation

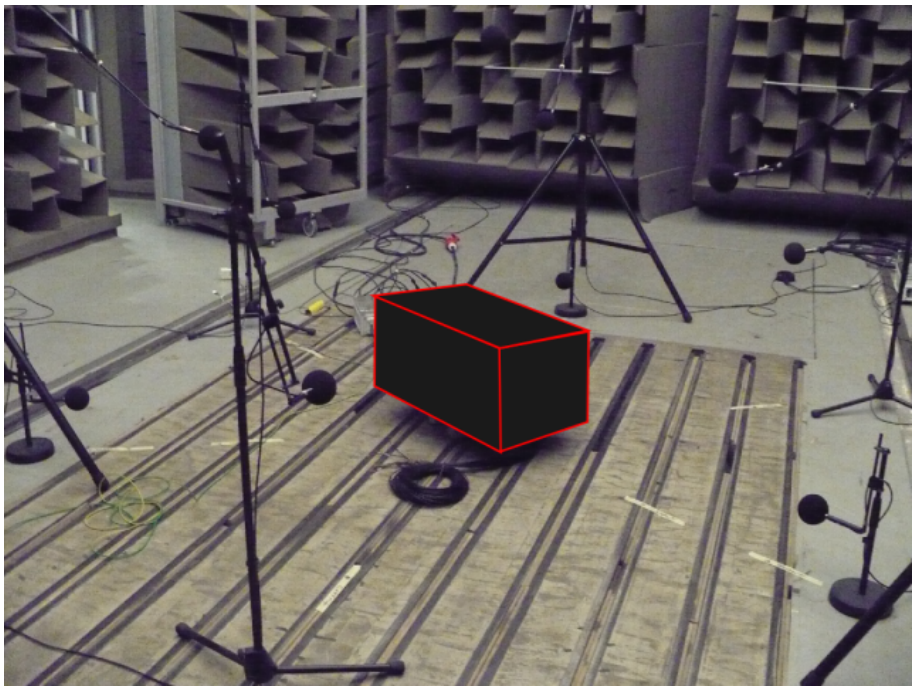

Figure 22: The test assembly at 60° rotation

5.4 Measurement equipment

The test equipment was centered around a HP (now Agilent) E1421B VXI Mainframe with E1432A input modules and a National Instruments MXI communication module. Data was collected with ten (10) Brüel & Kjær (B&K) 4189 free-field microphones with 2671 integrated circuit piezoelectric (ICP) preamplifiers. The microphone-preamplifier assemblies were calibrated on a B&K 4231 calibrator. Both the microphone-preamplifier assemblies and the sound calibrator were calibrated at accredited facilities within the year preceding the measurements. Measurement data was collected in NX I-deas Test suite, where preliminary preprocessing was undertaken to yield one-third-octave band figures for each measurement. Raw spectra for each microphone were also collected for further analysis in Excel acoustic measurement worksheets and more specific MATLAB analysis.

5.5 The testing plan

The measurements consisted of three steps:

1. Record background noise levels with the microphone assembly in place to determine background noise correction term K_1

2. Record reference sound source noise levels in all orientations to determine

environmental correction term K_2

3. Record all required test cases for the DUT

To recount, the goals of this thesis were threefold:

1. To determine how much noise is due to the cooling fans, how much due to chokes, and how much due to everything else
2. To determine whether and to which extent the noise output of the device exhibits variation due to voltage or power changes
3. To determine what the noise emissions of on-market devices are and what kind of variability they exhibit

To accomplish the above goals, the DUT was recorded at each operating point in all orientations. Then, the DUT was partially disassembled to remove the choke array. Following that, the device was recorded without the chokes in the test chamber, and subsequently the choke alone was placed into the test chamber and the rest of the inverter removed from it. Finally, each of the on-market devices was recorded at each operating point at 0° rotation. The operating points, where applicable, were as follows:

1. Idling, or 0 W power output
2. Full power at highest possible voltage
3. Intermediate power and voltage stages wherever deemed necessary

When all results were obtained, each measurement series (10 spectra, one from each microphone) was applied one-third octave smoothing. For each operating points, all 40 microphone positions were averaged for a surface-average noise level in both raw and smoothed spectra. Both unsmoothed and smoothed spectra were exported as plain text files for further analysis. Smoothed surface-average spectra were input into an Excel worksheet to yield noise emission values as per ISO 3744 (2010).

6 Research results

The measurement consisted of three stages. First, the adequacy of the test environment was determined by performing a series of preliminary measurements without any actual DUTs. Second, a comprehensive series of measurements was carried out on the Generic Device. Then, the GD was partially disassembled to remove the choke array, and the measurement suite repeated on both the device sans the choke and the choke array itself. Finally, select measurements were performed on eight on-market devices to test their noise emissions.

6.1 Preliminary measurements

The first stage of the measurement process was to measure the performance of the room. First, the level of background noise was determined, and then the level of environmental correction needed was determined by running a RSS and comparing recorded sound power levels against known sound power levels.

6.1.1 Background noise

Background noise for the room was determined by assembling the microphone array at the specified measurement distance and running the measurement without any active sound sources. The resulting average of background noise level spectra across all microphone positions is illustrated in Figure 23.

6.1.2 Reference sound source

After the surface average background noise level was determined, the reference sound source was used as the DUT. The RSS was run at all four rotations at a sound power level of 85 dB. The average environmentally uncorrected, unweighted sound power spectrum determined from all 40 microphone positions is shown in Figure 24. The recorded sound power level was then compared with the known sound power level to yield K_2. Both sound power levels and the resultant correction term are listed in Table 4.

Table 4: Determination of environmental correction term K_2

L_W^*	$L_{W,(\mathrm{RSS})}$	K_2
84.23	85.0	-0.77

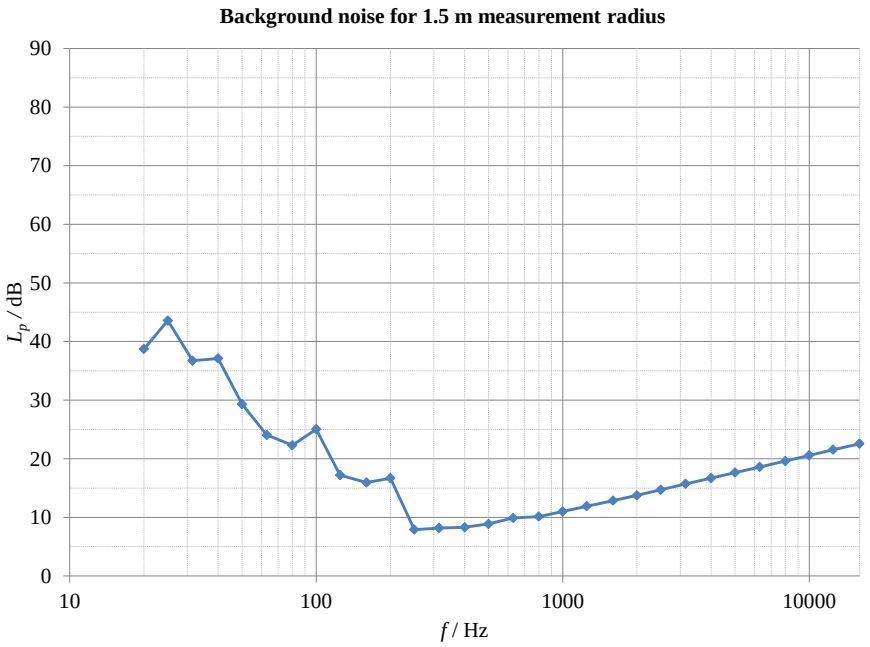

Figure 23: Background noise average unweighted sound pressure spectrum for 1.5 m measurement radius.

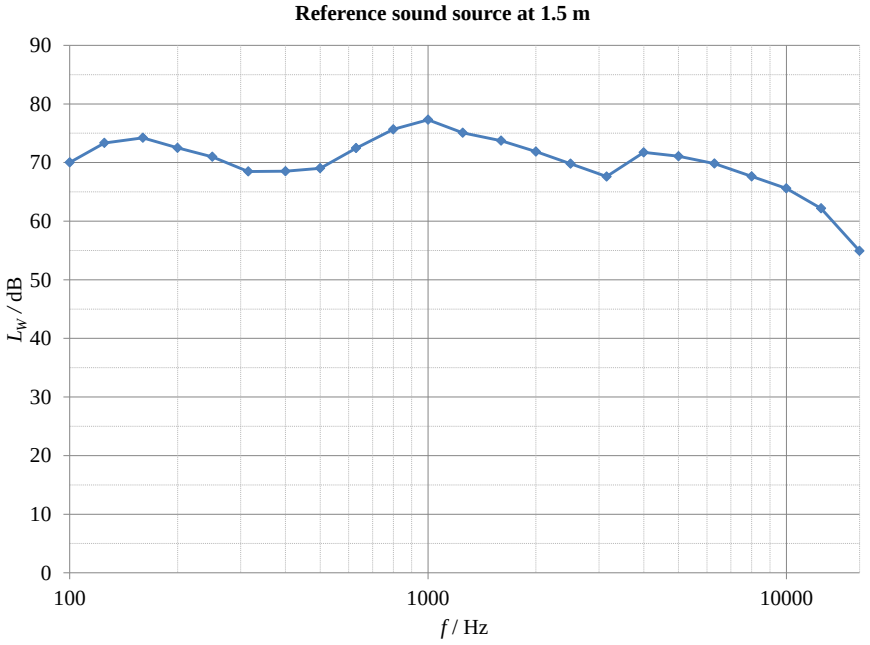

Figure 24: B&K 4205 reference sound source background noise corrected unweighted sound power spectrum for 1.5 m measurement radius.

6.2 Generic Device

The first device to be measured was the Generic Device. This device was run at all operating points at all four rotations. First, the GD was tested in its original condition. Second, the choke assembly was taken outside the test chamber, and the GD was run at all operating points without the choke. Then, the choke assembly was placed as the DUT and the GD was taken outside the chamber. All measurements were then repeated on the choke assembly. In the first two cases, the cooling fan was switched off for the cases where a fanless condition is implicated.

6.2.1 Generic Device with choke assembly

First, the GD was run as a full assembly. The 40-point surface average sound power spectra for all operating points are illustrated in Figure 25. The corresponding single-number noise emission values are presented in Table 5.

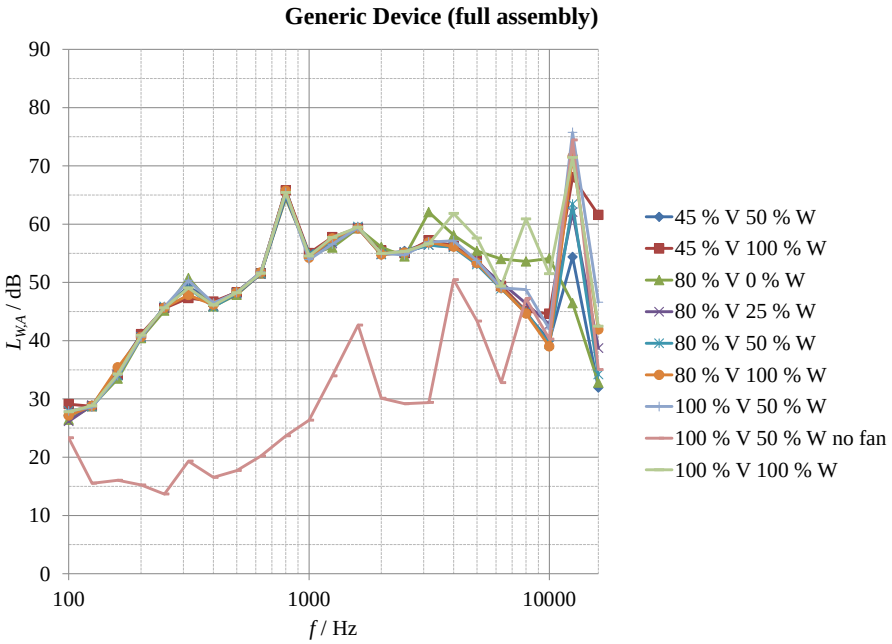

Figure 25: Generic Device (full assembly) sound power spectra.

6.2.2 Generic Device without choke assembly

After the measurements with the full GD assembly were completed, the choke assembly was removed from the chassis. Then, sufficiently long electrical cables were installed between the choke and the rest of the device to ensure the normal electrical operation of the GD. The choke assembly was then taken outside the test chamber

Table 5: Generic Device full assembly single-number noise emission values

Operating point	$L_{W,A}$	$L_{W,A,16k}$	$L_{W,A,ext}$
45 % voltage 50 % power	68.9	54.4	69.1
45 % voltage 100 % power	69.0	68.9	72.0
80 % voltage 0 % power	69.4	46.6	69.5
80 % voltage 25 % power	68.4	62.1	69.3
80 % voltage 50 % power	68.5	63.4	69.7
80 % voltage 100 % power	68.8	71.6	73.5
100 % voltage 50 % power	68.8	75.7	76.5
100 % voltage 50 % power without fan	53.5	74.4	74.5
100 % voltage 100 % power	70.1	71.4	73.8

so the rest of the GD could be run as the DUT. The results of this batch are given in Figure 26 and Table 6.

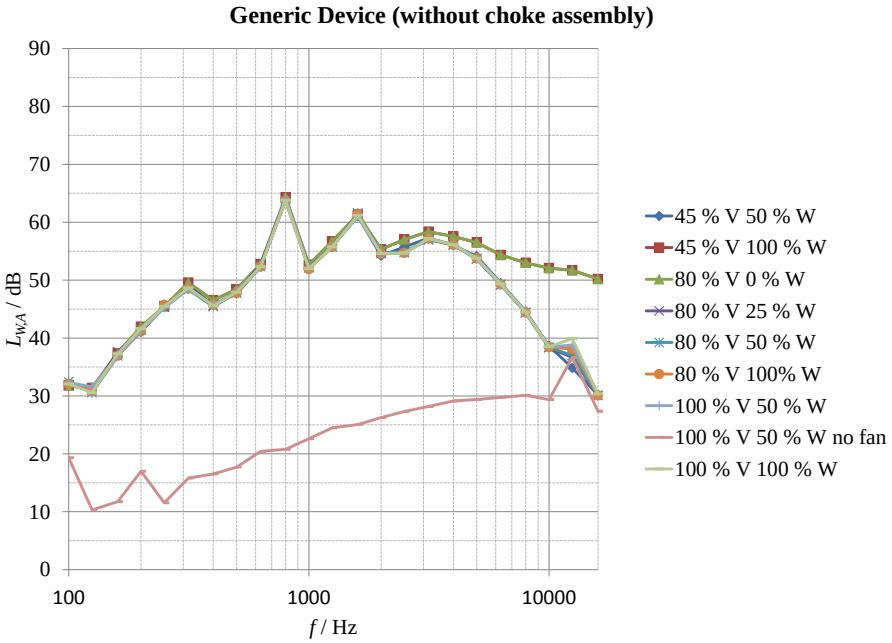

Figure 26: Generic Device (without choke assembly) sound power spectra.

6.2.3 Choke assembly only

Finally, the placement of the GD and its choke assembly were reversed, so the chokes resided in the test chamber and the GD in the lobby. The standard batch of measurements, with the exception of the fanless condition, were repeated with this setup. The results of this measurement series are given in Figure 27 and Table 7.

Table 6: Generic Device without choke assembly single-number noise emission values

Operating point	$L_{W,A}$	$L_{W,A,16k}$	$L_{W,A,ext}$
45 % voltage 50 % power	68.2	36.1	68.2
45 % voltage 100 % power	69.2	54.0	69.3
80 % voltage 0 % power	69.2	54.0	69.3
80 % voltage 25 % power	68.3	37.5	68.3
80 % voltage 50 % power	68.2	37.8	68.2
80 % voltage 100 % power	68.2	38.8	68.2
100 % voltage 50 % power	68.2	39.4	68.2
100 % voltage 50 % power without fan	38.7*	37.1	41.0*
100 % voltage 100 % power	68.1	40.4	68.1

* Value does not conform to ISO 3744 requirements on background noise

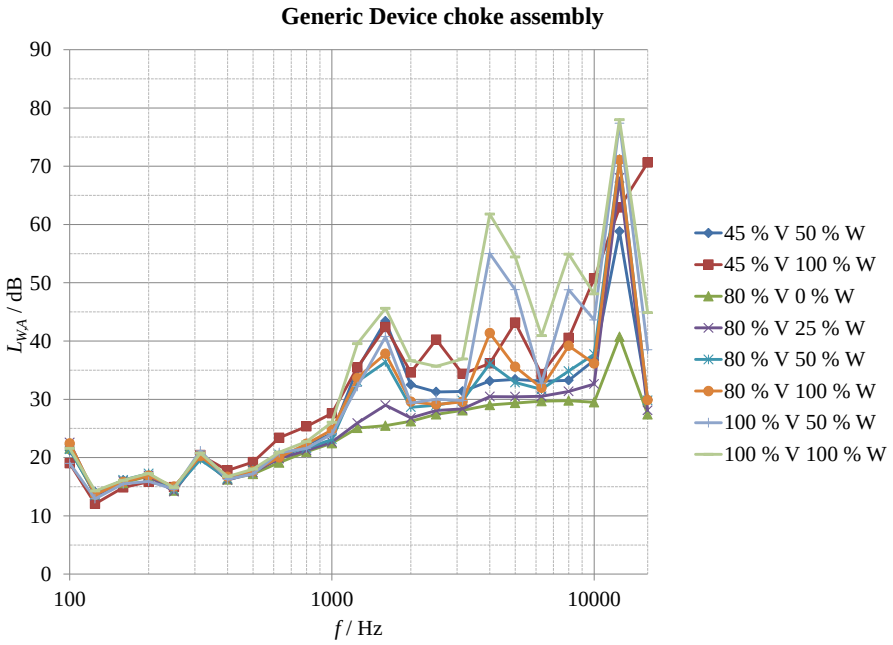

Figure 27: Generic Device choke assembly sound power spectra.

Table 7: Generic Device choke assembly single-number noise emission values

Operating point	$L_{W,A}$	$L_{W,A,16k}$	$L_{W,A,ext}$
45 % voltage 50 % power	46.4*	58.8	59.1
45 % voltage 100 % power	52.9	71.3	71.4
80 % voltage 0 % power	38.8*	40.9	43.0*
80 % voltage 25 % power	40.2*	68.0	68.0
80 % voltage 50 % power	44.2*	71.2	71.2
80 % voltage 100 % power	46.4*	71.1	71.1
100 % voltage 50 % power	57.1	77.4	77.4
100 % voltage 100 % power	63.5	78.0	78.1

* Value does not conform to ISO 3744 requirements on background noise

6.3 On-market devices

In the third stage of the measurements, a total of eight on-market devices were run at various operating points. This batch of devices, however, was run only at one orientation. The measurements in this section are presented in alphabetical order, as opposed to chronological order.

6.3.1 Danfoss TLX 15

The first device in this batch was Danfoss TLX 15, a 15 kW device. It was run at two voltages and a variety of power outputs. The results are presented in Figure 28 and Table 8.

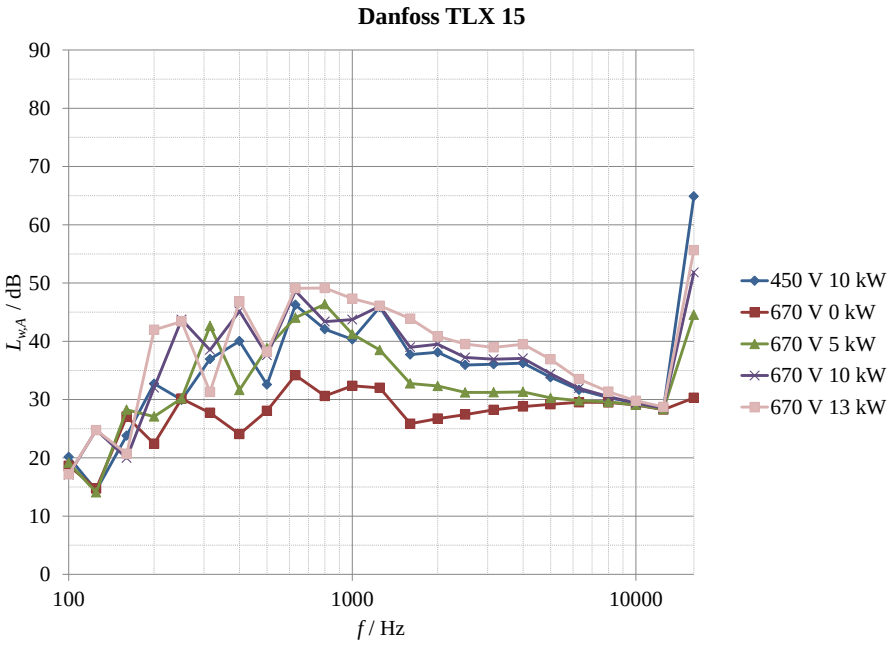

Figure 28: Danfoss TLX 15 sound power spectra.

Table 8: Danfoss TLX 15 single-number noise emission values

Operating point	$L_{W,A}$	$L_{W,A,16k}$	$L_{W,A,ext}$
450 V 10 kW	52.0	64.9	65.1
670 V 0 kW	42.2*	32.4*	42.6*
670 V 5 kW	51.1	44.6	52.0
670 V 10 kW	54.3	51.8	56.2
670 V 13 kW	56.3	55.7	59.0

* Value does not conform to ISO 3744 requirements on background noise

6.3.2 Fronius IG TL 5.0

The second device is Fronius IG TL 5.0, a transformerless 5 kW device. It was run only at the maximum power condition at two different voltages. The results are given in Figure 29 and Table 9.

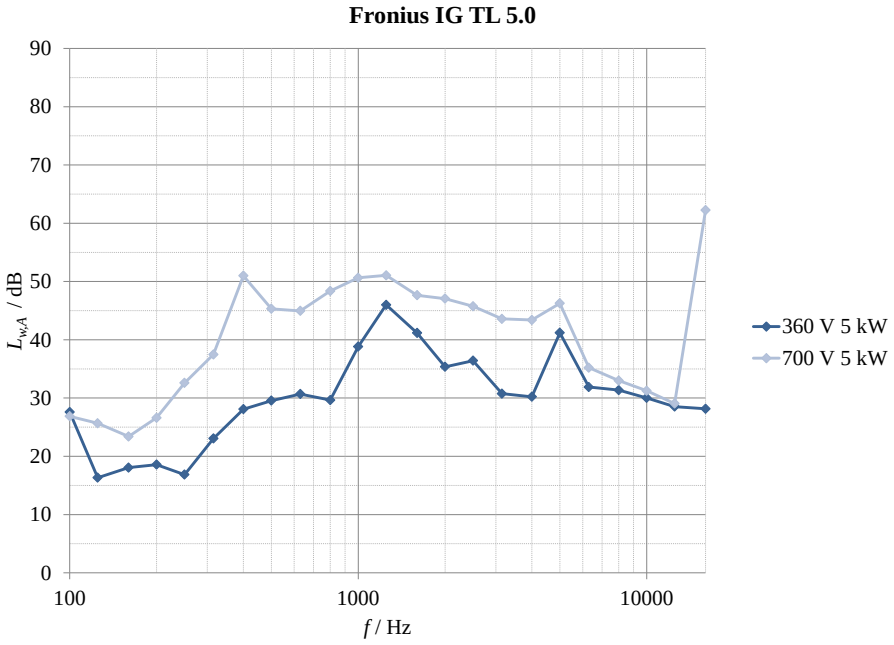

Figure 29: Fronius IG TL 5.0 sound power spectra.

Table 9: Fronius IG TL 5.0 single-number noise emission values

Operating point	$L_{W,A}$	$L_{W,A,16k}$	$L_{W,A,ext}$
360 V 5 kW	49.6	31.4*	49.7
700 V 5 kW	58.8	62.2	63.9

* Value does not conform to ISO 3744 requirements on background noise

6.3.3 Kostal PIKO 8.3

The third device is Kostal PIKO 8.3, a 8.3 kW inverter. It was run at three different voltages, each at full power, and at two additional power conditions at 670 V. The results of these tests are given in Figure 30 and Table 10.

6.3.4 PowerOne Aurora Trio 20.0

Fourth, a 20 kW device, the PowerOne Aurora Trio 20.0, was tested. This device has the highest power rating of all the devices tested. It was run at three different

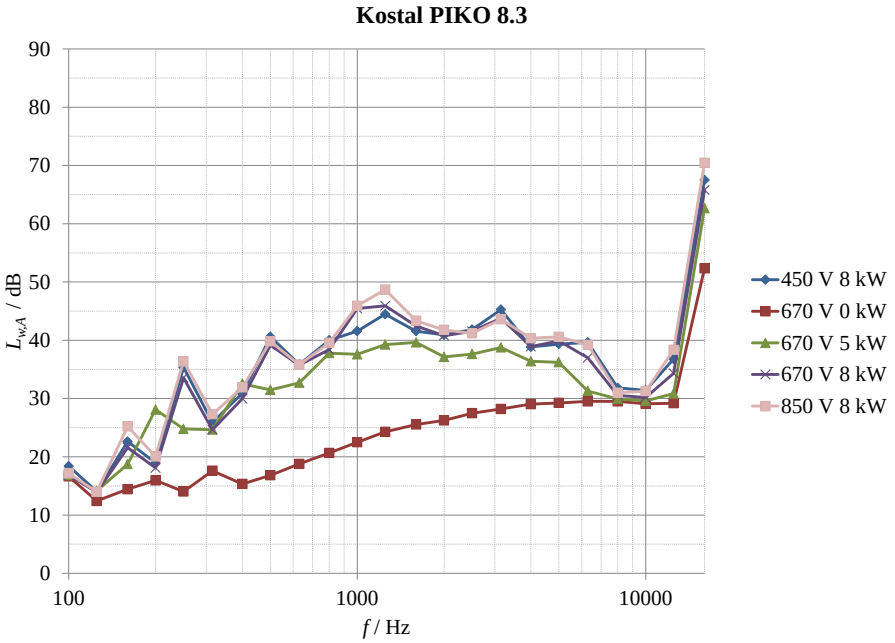

Figure 30: Kostal PIKO 8.3 sound power spectra.

Table 10: Kostal PIKO 8.3 single-number noise emission values

Operating point	$L_{W,A}$	$L_{W,A,16k}$	$L_{W,A,ext}$
450 V 8 kW	52.5	67.5	67.6
670 V 0 kW	38.6*	52.4	52.5
670 V 5 kW	48.2	62.7	62.8
670 V 8 kW	52.8	65.8	66.0
850 V 8 kW	54.0	70.5	70.6

* Value does not conform to ISO 3744 requirements on background noise

voltages, and four different power conditions. The sound power spectra are presented in Figure 31, and the corresponding single-number emission values in Table 11.

Table 11: PowerOne Aurora Trio 20.0 single-number noise emission values

Operating point	$L_{W,A}$	$L_{W,A,16k}$	$L_{W,A,ext}$
400 V 10 kW	48.6	77.1	77.1
670 V 0 kW	38.7*	54.6	54.7
670 V 5 kW	43.6*	67.0	67.1
670 V 10 kW	49.0	73.3	73.3
670 V 20 kW	59.5	78.3	78.3
800 V 20 kW	60.8	84.3	84.3

* Value does not conform to ISO 3744 requirements on background noise

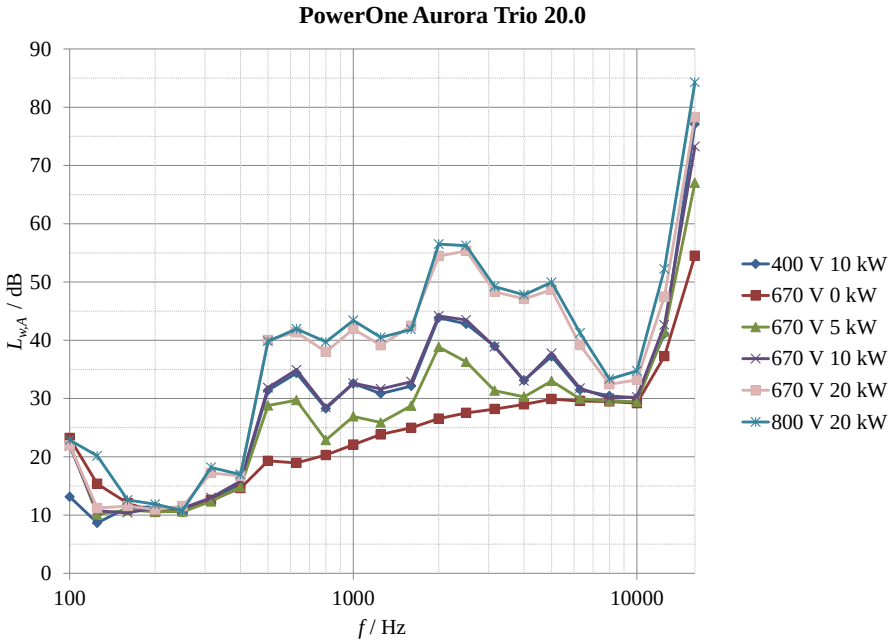

Figure 31: PowerOne Aurora Trio 20.0 sound power spectra.

6.3.5 PowerOne PVI-3.0

Next, another device by PowerOne, the PVI-3.0, was tested. This is a significantly lower powered device, and at 3 kW is the least powerful device in the batch. It was run only at the full power condition at two different voltages. The spectra are displayed in Figure 32, and the single-number emission values in Table 12.

Table 12: PowerOne PVI-3.0 single-number noise emission values

Operating point	$L_{W,A}$	$L_{W,A,16k}$	$L_{W,A,ext}$
260 V 3 kW	38.9*	33.0*	39.9*
530 V 3 kW	38.5*	30.6*	39.2*

* Value does not conform to ISO 3744 requirements on background noise

6.3.6 REFUsol 017K

The sixth case was another high-powered device, the 16.5 kW REFUsol 017k. This device was run at two voltages. The results are given in Figure 33 and Table 13.

6.3.7 SMA Sunny Tripower 6000TL

The seventh on-market device to be tested was another low-powered transformerless inverter, the 6 kW SMA Sunny Tripower 6000TL. This device, along with other low-

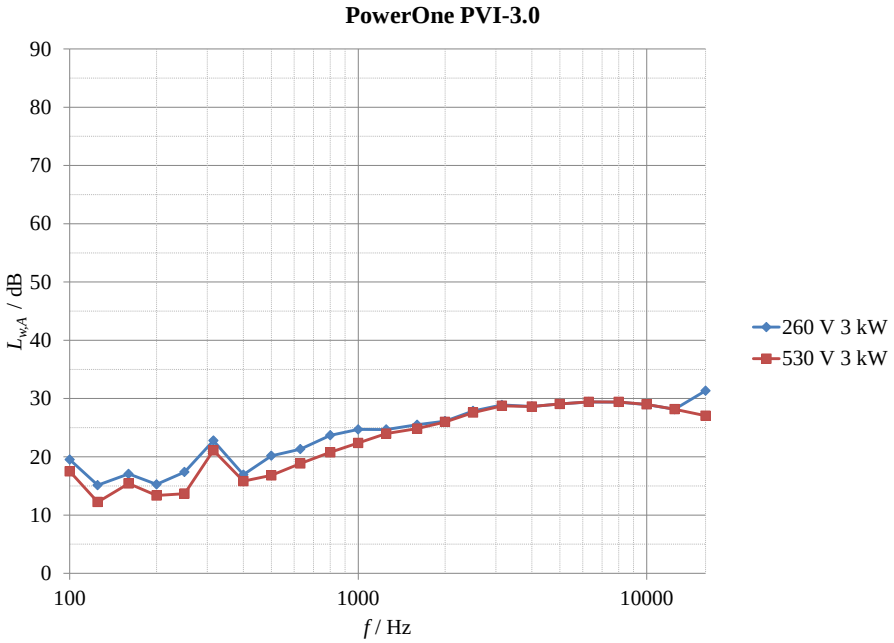

Figure 32: PowerOne PVI-3.0 sound power spectra.

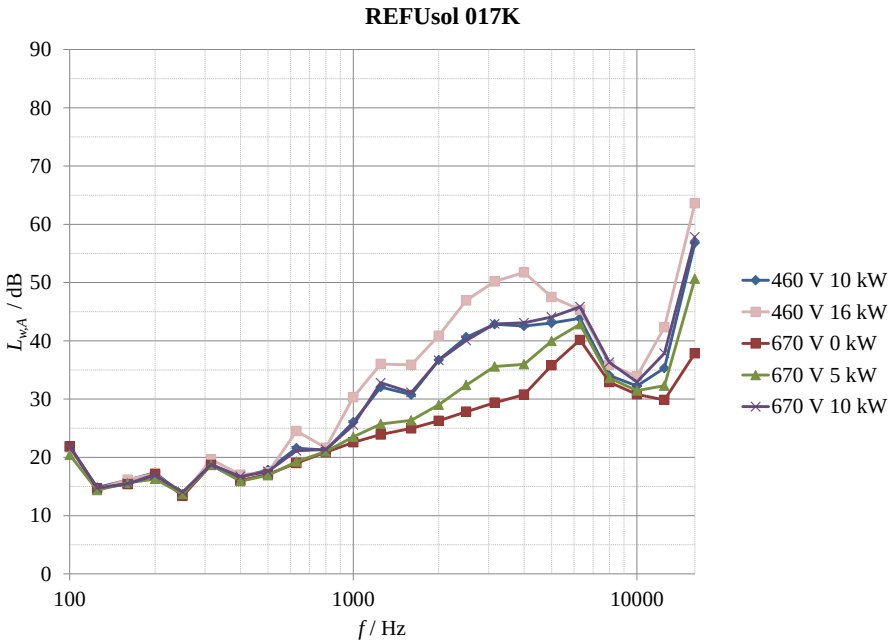

Figure 33: REFUsol 017K sound power spectra.

powered devices, was only run at the full power condition at two different voltages. The results are given in Figure 34 and Table 14.

Table 13: REFUsol 017K single-number noise emission values

Operating point	$L_{W,A}$	$L_{W,A,16k}$	$L_{W,A,ext}$
460 V 10 kW	50.3	56.8	57.7
460 V 16 kW	56.2	63.6	64.4
670 V 0 kW	43.4*	38.5*	44.6*
670 V 5 kW	46.5*	50.7	52.1
670 V 10 kW	51.1	57.9	58.7

* Value does not conform to ISO 3744 requirements on background noise

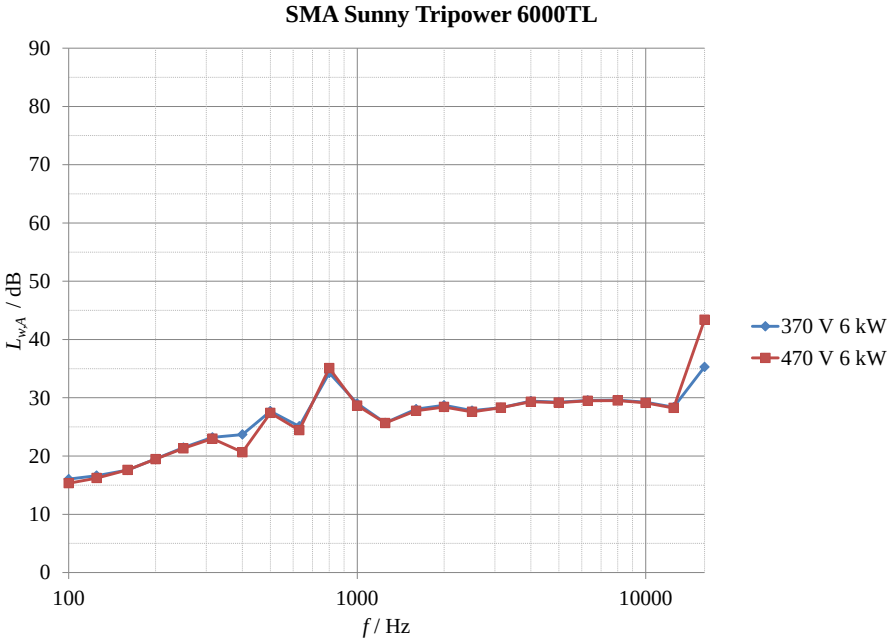

Figure 34: SMA Sunny Tripower 6000TL sound power spectra.

Table 14: SMA Sunny Tripower 6000TL single-number noise emission values

Operating point	$L_{W,A}$	$L_{W,A,16k}$	$L_{W,A,ext}$
370 V 6 kW	41.0*	36.1*	42.2*
470 V 6 kW	41.0*	43.5	45.4*

* Value does not conform to ISO 3744 requirements on background noise

6.3.8 Voltwerk VS 15

The final device to be tested was Voltwerk VS 15, a 15 kW inverter. It was operated at three different voltages and a variety of power conditions. The sound power spectra of the device are presented in Figure 35. The associated single-number noise emission values are given in Table 15.

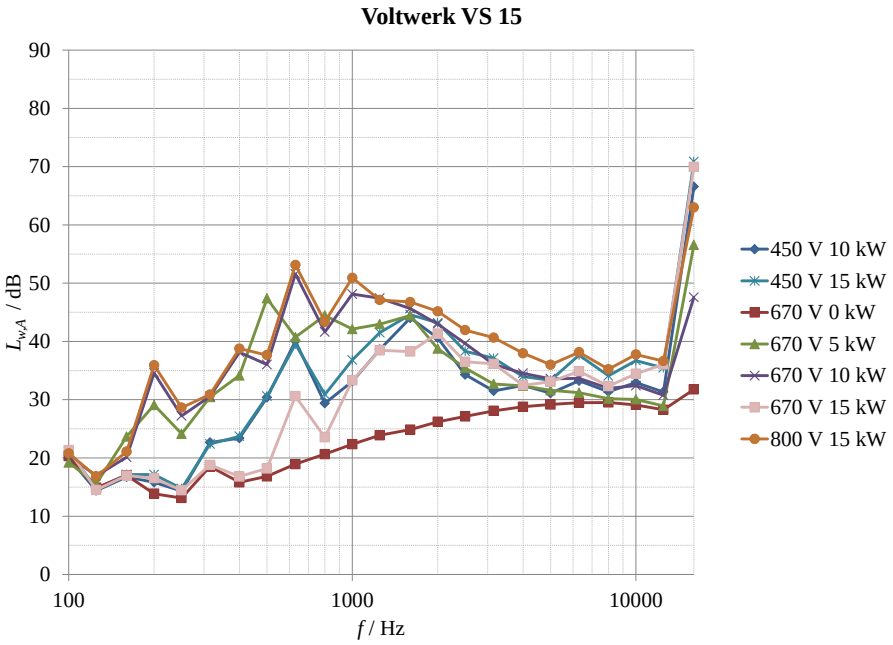

Figure 35: Voltwerk VS 15 sound power spectra.

Table 15: Voltwerk VS 15 single-number noise emission values

Operating point	$L_{W,A}$	$L_{W,A,16k}$	$L_{W,A,ext}$
450 V 10 kW	48.5*	66.6	66.6
450 V 15 kW	50.4	70.8	70.9
670 V 0 kW	38.5*	33.4*	39.7*
670 V 5 kW	52.6	56.6	58.0
670 V 10 kW	55.7	47.7	56.4
670 V 15 kW	47.1*	70.0	70.0
800 V 15 kW	57.4	63.0	64.1

* Value does not conform to ISO 3744 requirements on background noise

7 Analysis of results

7.1 Validity of results

All measured devices conform to the requirement that measurement radius $r \geq 2d_O$.

The environmental correction term K_2 turned out to be negative (Table 4, Page 40). This means that less sound energy is being recorded by the microphones than is produced by the sound source. This might mean a defect in the calibration of any of the devices in the measurement chain (microphones, preamplifiers, microphone interfaces, reference sound source, sound level meter), or that the floor of the measurement space is not entirely reflective, or that the source does not radiate sound uniformly enough. But then again, the measured value is well within measurement uncertainty, so it is possible that it is a product of random error.

The environmental correction term K_2 was determined as a single A-weighted figure as opposed to individual measurements on frequency bands. This was because the reference sound source was only able to provide sound up to 10 kHz. Also, the device had only octave-band filters pre-installed, so measurements in one-third-octave bands was not possible without additional equipment. Thus, it was decided that the A-weighted figure should be seen as representative of the room as a whole on the entire spectrum. Measurement in one-third-octave bands up to 20 kHz would have been preferable, but was precluded by the available equipment.

Of measured noise emission levels, there are deficiencies in background noise clearance. For on-market devices, 27 measured levels out of 102 do not satisfy ISO 3744 requirements on ΔL_p, for a rate of 26.5%. Of measurements performed on the Generic Device and its sub-assemblies, 8/78 measurements fail to satisfy said requirements, for a rate of 10.3%. For the entire batch, 35/180 were invalidated by this criterion, for a rate of 19.4%.

Additionally, all measurements fail to satisfy ISO 3744 criteria due to the fact that a post-measurement calibration was not performed on the measurement instrumentation.

7.2 Noise source analysis of Generic Device

7.2.1 Noise component analysis

Figure 36 illustrates the measured effects of assumed noise sources on the sound power emissions of the device. As can be seen, the noise emissions of the full assembly track almost perfectly with the emissions of the assembly sans choke up until the 6.3 kHz one-third-octave band. From that frequency onward, the full-

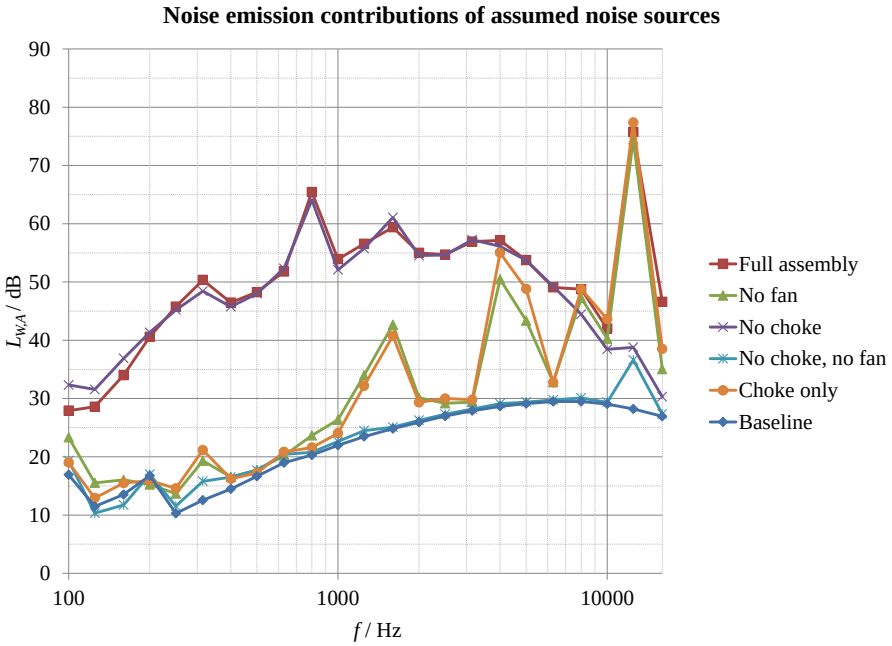

Figure 36: Noise component analysis of Generic Device at 100% voltage and 50% power.

assembly emissions track remarkably closely with both the fanless assembly and the solitary choke assembly.

It is also quite remarkable, that the solitary choke assembly tracks very closely with the fanless assembly, with significant deviations only at the 4 kHz and 5 kHz bands. This suggests, contrary to initial assumptions, that the choke assembly primarily emits airborne noise, as opposed to structural noise. It is also possible, although quite unlikely (at least in this author's appraisal), that any reductions in airborne noise resulting from the installation of the choke assembly into the chassis are offset by the addition of structural sources of sound.

The "baseline" series in the diagram is the measurement of silence, converted into an A-weighted sound power series using the same constants as for actual measurements. As can be seen, the level rises steadily, and the rate of change diminishes as frequency increases. This is an artefact of both increasing filter bandwidth (a rise of 3 dB per octave, or 1 dB per one-third-octave) and A-weighting (de-emphasizing frequencies outside 1 kHz and 4 kHz). If we assume a spectrally white distribution of sound, this is exactly the kind of figure we would anticipate. Thus, in the measurement setup, we can deduce that background noise distribution is essentially white above the 250 Hz band.

When we compare this baseline noise figure with the minimal assembly (i.e. the Generic Device without either fan or choke), it can be observed that it is essen-

tially soundless, except for very minor perturbations below 1 kHz and a significant peak at the 12.5 kHz band. This is congruent with the assumption that the device contains some additional power electronic components that produce noise at modulating frequencies. However, these components' noise emissions pale in comparison with the emissions of the choke: the level difference is in the order of 40 dB.

Thus, the overarching conclusions of this component analysis is that for frequency bands of 6.3 kHz and under, noise contributions are due to the cooling fan, for frequency bands of 12.5 kHz and over, the noise emissions are almost exclusively due to the choke assembly. For the frequency bands of 8 and 10 kHz, the noise emissions represent a mixture of fan and choke noise.

7.2.2 Voltage-related variability of noise emission

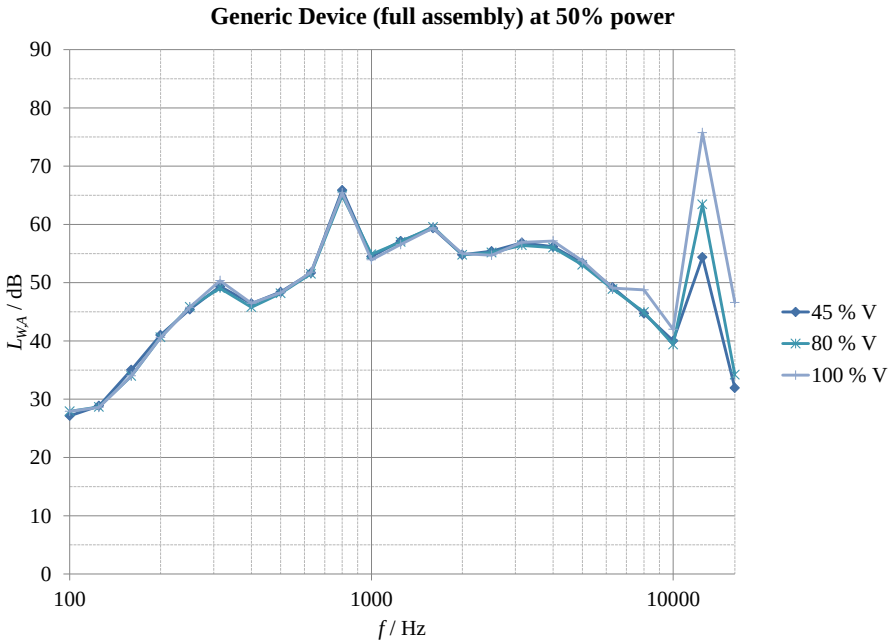

Figure 37: Voltage-related variability of noise emission of Generic Device full assembly at 50 % power.

Figure 37 illustrates the voltage-related change in noise emissions of the full Generic Device. It is clearly evident, that except for the 12.5 kHz and 16 kHz bands, the device exhibits very minor variations in sound emission. As discussed above, these bands' emissions are almost exclusively due to choke noise. Thus, it seems that variations in choke noise output are primarily voltage-dependent.

The significance of choke noise is further corroborated by the data in Figure 38. Without the choke, the only voltage-dependent variations in noise emissions are

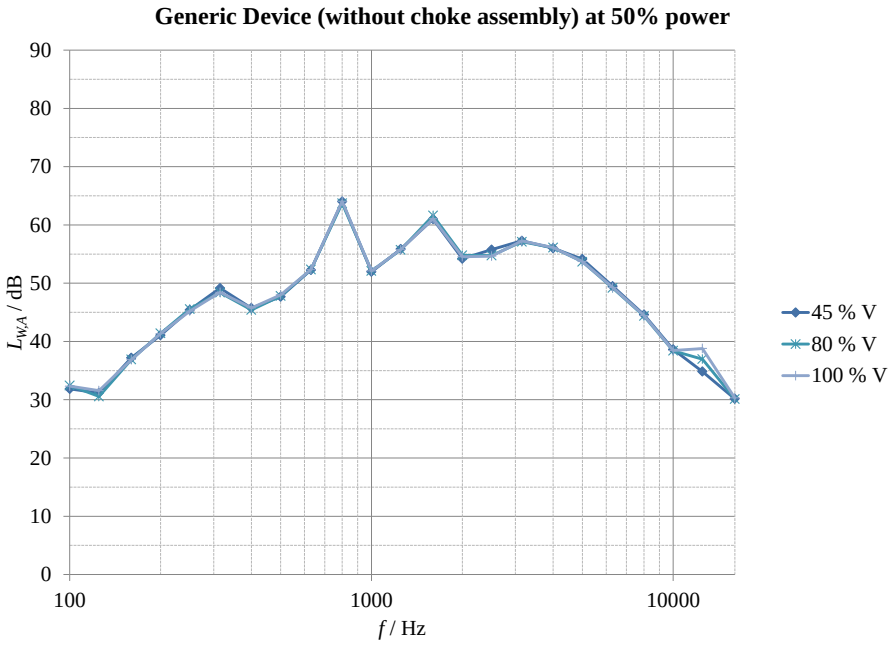

Figure 38: Voltage-related variability of noise emission of Generic Device without choke assembly at 50 % power.

slight disturbances at the 12.5 kHz band, probably due to additional components operating at the modulation frequency.

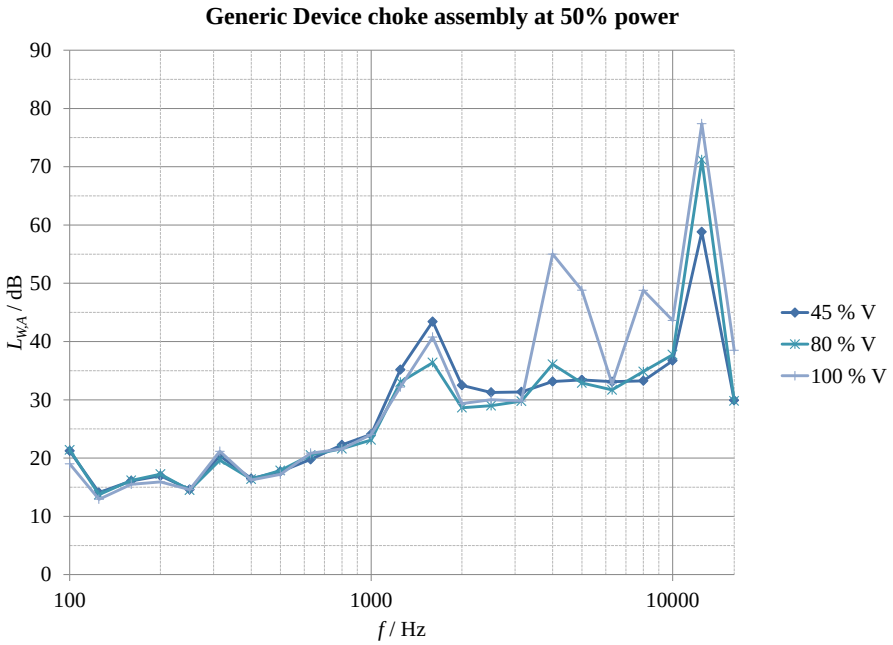

Figure 39: Voltage-related variability of noise emission of Generic Device choke assembly at 50 % power.

Figure 39 illustrates how voltage variations produce variations in noise emissions in the choke assembly alone. As expected, variations at the 12.5 kHz band align with variations in voltage. However, additional peaks at 4 kHz, 5 kHz and 8 kHz present themselves only at the highest voltage level. The reason for this is unclear, although it is possible that this is due to the saturation effect of magnetostriction. Curiously, at frequencies between 1.25 kHz and 3.15 kHz, the lowest voltage level is associated with the highest sound emission level. The reason for this is entirely unclear.

7.2.3 Power-related variability of noise emission

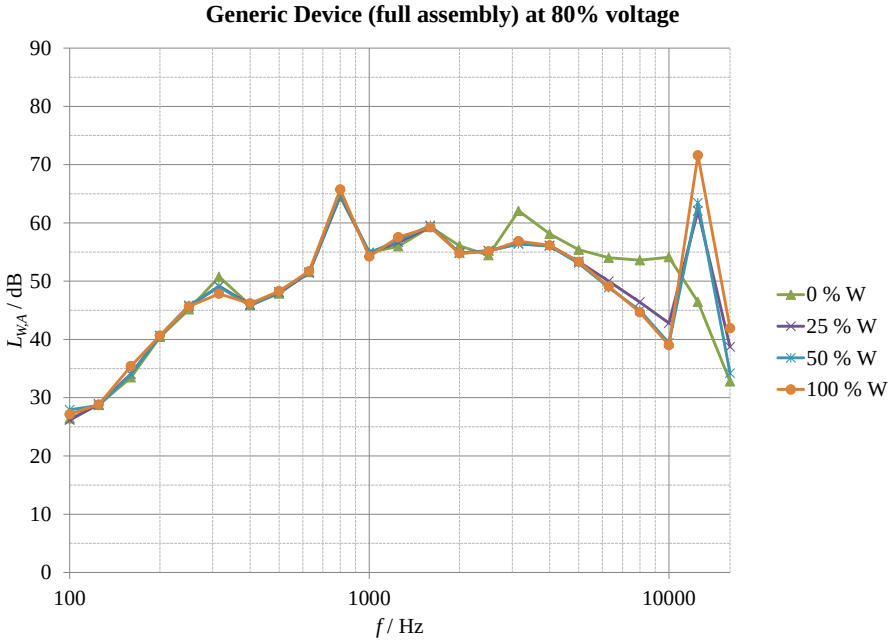

Figure 40: Power-related variability of noise emission of Generic Device full assembly at 80 % voltage.

Illustrated in Figure 40 is the power-related variation in noise emission for the full Generic Device assembly. At frequencies of 2.5 kHz and below, there is essentially no power-related variation. At the 12.5 and 16 kHz bands, there is a modulation scheme based variation in noise emission, similar to voltage-related variability. However, at frequencies between 3.15 kHz and 10 kHz, there is a curious inverse relationship between power and noise emission. This could be called an *idling artefact*. It seems to disappear for all power-carrying operating points, except for 25% power at 8 kHz and 10 kHz. However, this discrepancy is minor, and is close to measurement uncertainty. It could be that this idling artefact exhibits a frequency-dependent saturation curve with regard to power. A similar, although lesser inverse relationship can be observed at 315 Hz.

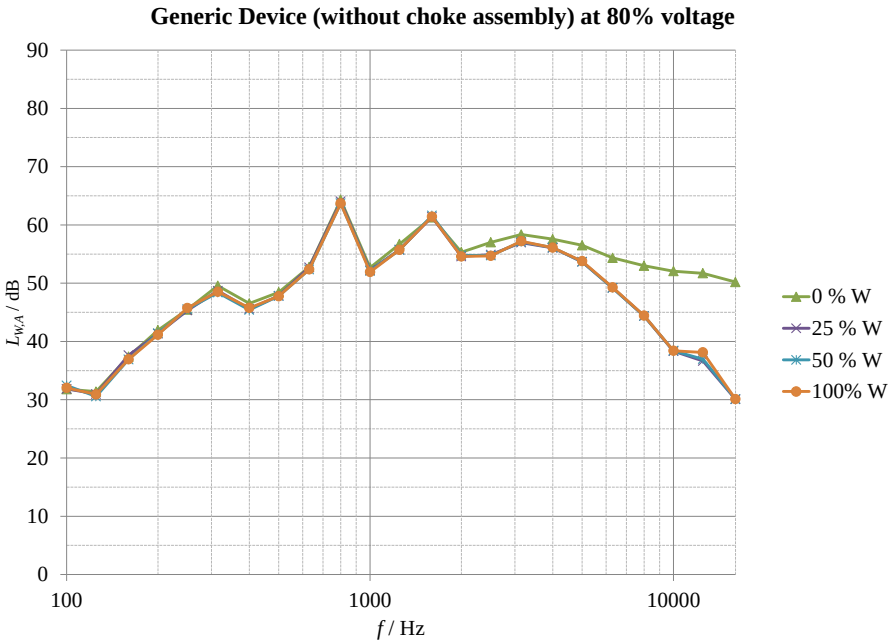

Figure 41: Power-related variability of noise emission of Generic Device without choke assembly at 80 % voltage.

This inverse relationship is further illustrated in Figure 41. With the elimination of the choke assembly, nearly all power-related variations disappear. The only exception is the idling artefact exhibited at frequency bands of 2.5 kHz and over, with significance increasing with frequency.

The power-related variations of the choke assembly are illustrated in Figure 42. At modulation frequencies, there is a significant rise in noise emission with regard to power, although there is little difference between 25, 50 and 100 % power. Power-related differences are accentuated at frequencies below modulation frequency. The peaks at 1.6 kHz, 4 kHz and 8 kHz exhibit a clear direct relationship between power and noise emission. The peak at 1.6 kHz seems to saturate earlier than the peaks at 4 kHz and 8 kHz.

The relative constancy of power-dependent noise emission at frequencies below 10 kHz seems to suggest that the cooling fan is always on. It is quite probable that the implementation of a varying-speed cooling fan would reduce noise emissions below the switching frequency. Judging from Table 25 (on Page 42), the noise emission below 10 kHz would fall 15.5 dB by the removal of the fan, leading us to believe that fan-borne noise emissions vary by up to this amount. However, since the most significant source of noise is the choke assembly, the wholesale elimination of the cooling fan reduces total noise emission only by 2.0 dB.

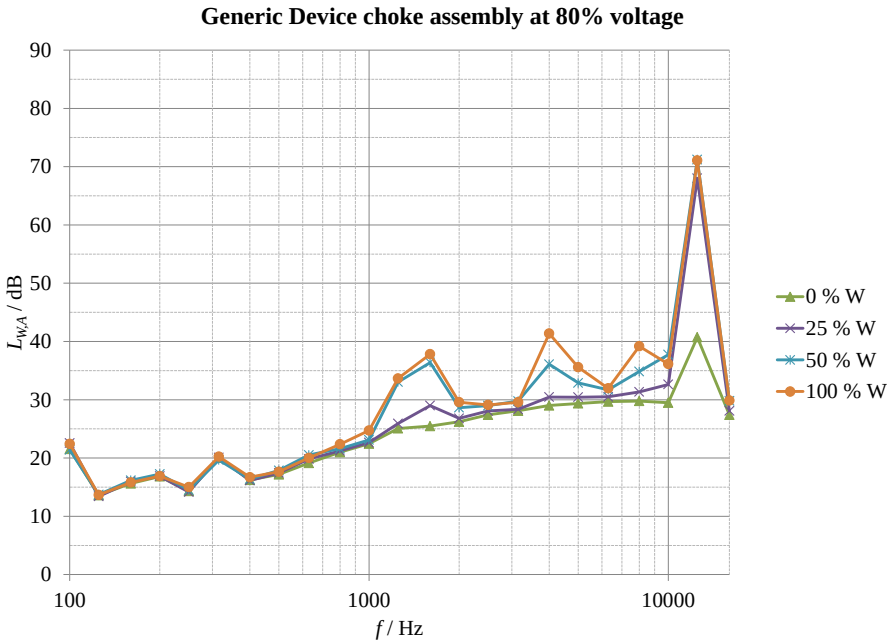

Figure 42: Power-related variability of noise emission of Generic Device choke assembly at 80 % voltage.

7.3 Noise emissions of on-market devices

7.3.1 Congruence with declared noise emission values

The comparison of manufacturer stated noise emission values with measured values is not a trivial task. None of the manufacturers even state which noise emission quantity is reported, let alone the methods by which they were obtained. A reasonable assumption, based on conventions in popular literature, is that these figures essentially represent A-weighted sound pressure values measured from a set distance, typically 1 m. It can also be assumed that this A-weighted value only includes the frequency band within 100 Hz and 10 kHz.

Table 16: Declared versus measured noise emission values of on-market devices. Measurement uncertainty was ±3 dB.

Device	Declared noise emission	$L_{W,A}$	$L_{p,A,1m}$	$L_{W,A,ext}$	$L_{p,A,1m,ext}$
Danfoss TLX 15	max. 56 dB(A)	56.3	43.3	59.0	46.0
Fronius IG TL 5.0	N/A	58.8	46.2	63.9	51.3
Kostal PIKO 8.3	33...46 dB(A)	54.0	41.4	70.6	58.0
PowerOne Aurora Trio 20.0	< 50 dB(A) @ 1 m	60.8	47.2	84.3	70.7
PowerOne PVI-3.0	< 50 dB(A) @ 1 m	38.9	26.3	39.9	27.3
REFUsol 017K	< 45 dBA	56.2	43.2	64.4	51.4
SMA Sunny Tripower 6000TL	40 dB(A) (typical)	41.0	28.1	45.4	32.5
Voltwerk VS 15	N/A	57.4	44.4	64.1	51.1

As can be seen from Table 16, only PowerOne PVI-3.0's measured sound power falls below the declared value. Danfoss TLX 15 comes within measurement uncertainty of its declared noise emission value, and SMA 6000TL comes within measurement uncertainty if we restrict the observed band's upper limit to 10 kHz. If we assume all declarations represent emission sound pressure levels, and restrict bandwidth, all measured devices perform as declared.

However, it is more prudent to consider all noise emissions as sound power levels, as sound pressure levels can vary considerably in the field surrounding the device. Also, with regards to human perception, all audible frequencies should be considered as contributing to overall noise emission levels, as is suggested in ISO 7779. When this is done, measured sound power levels rise remarkably. Only the PowerOne PVI-3.0 remains well below measured noise emissions. The differences between declared noise emission levels and measured, perceptible noise levels are outlined in Table 17.

Table 17: Difference between noise emission declarations and actual sound power levels.

Device	Level difference
Danfoss TLX 15	3.0
Kostal PIKO 8.3	24.6
PowerOne Aurora Trio 20.0	34.3
PowerOne PVI-3.0	-10.1
REFUsol 017K	19.4
SMA Sunny Tripower 6000TL	5.4

As outlined in Table 17, only PowerOne PVI-3.0 is true to declared noise emission levels, and Danfoss TLX 15 comes within measurement uncertainty. All other devices, for which a noise emission level was declared, differ considerably, even by over 30 dB. This is a staggering discrepancy, and it should be obvious, that there needs to be a more fitting measurement standard for this family of devices.

7.3.2 Voltage-related variability of noise emissions

Danfoss TLX 15 (Figure 43) displays a dichotomy of voltage-related noise emission variability: lower-frequency sound emission increases with voltage, whereas high-frequency noise (at the 16 kHz band) decreases with voltage, suggesting instead a current-related increase in noise emissions.

Fronius IG TL 5.0 (Figure 44), on the other hand, shows prominent voltage-related rises in noise emissions throughout the frequency spectrum.

Contrasted with both above devices, Kostal PIKO 8.3 (Figure 45) shows no

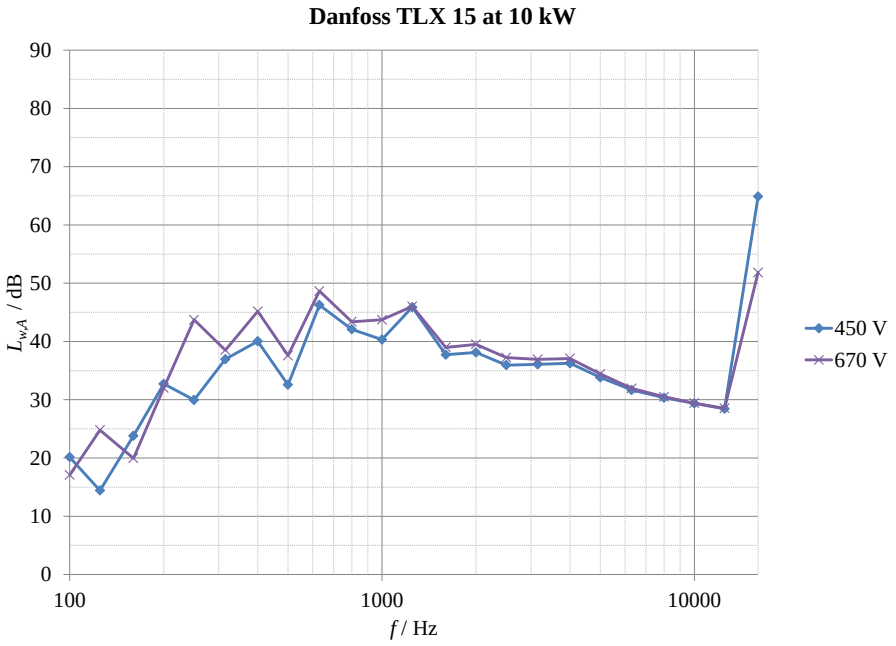

Figure 43: Voltage-related variability of noise emission of Danfoss TLX 15 at 10 kW.

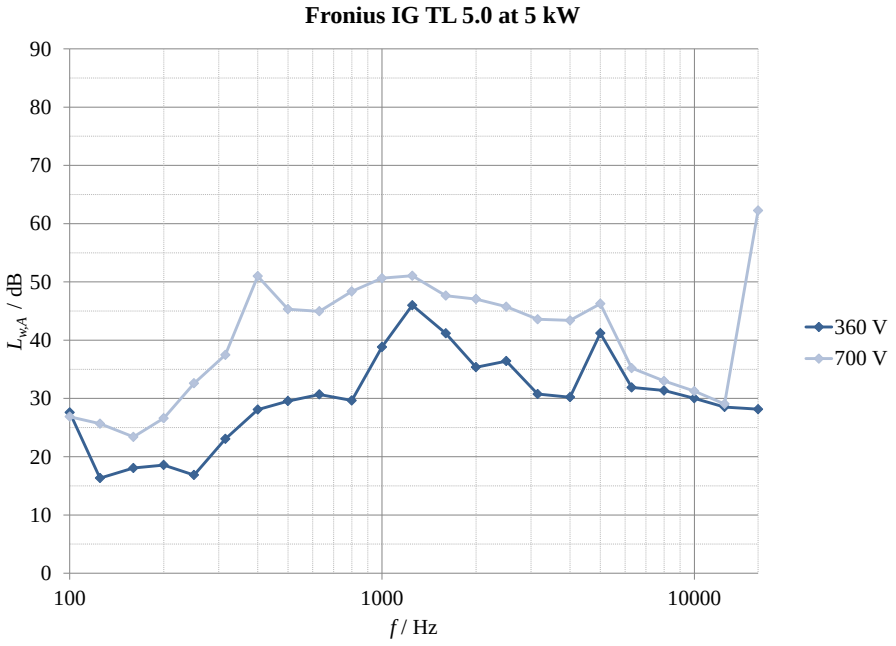

Figure 44: Voltage-related variability of noise emissions of Fronius IG TL 5.0 at 5 kW.

significant variations in any frequency range.

PowerOne Aurora Trio 20.0 (Figure 46) exhibits almost the same behaviour, differing only at the 100 Hz band. This corresponds to the second harmonic fre-

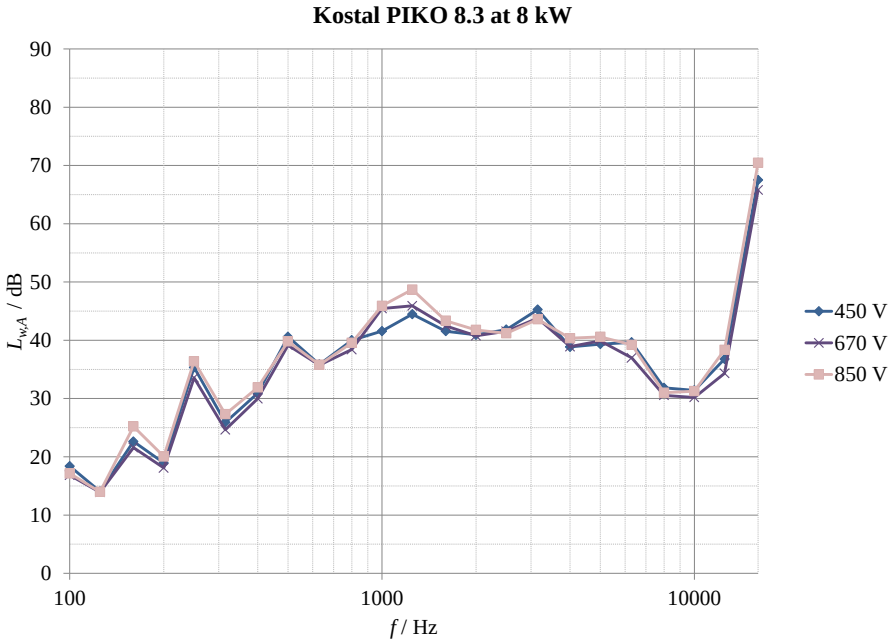

Figure 45: Voltage-related variability of noise emissions of Kostal PIKO 8.3 at 8 kW.

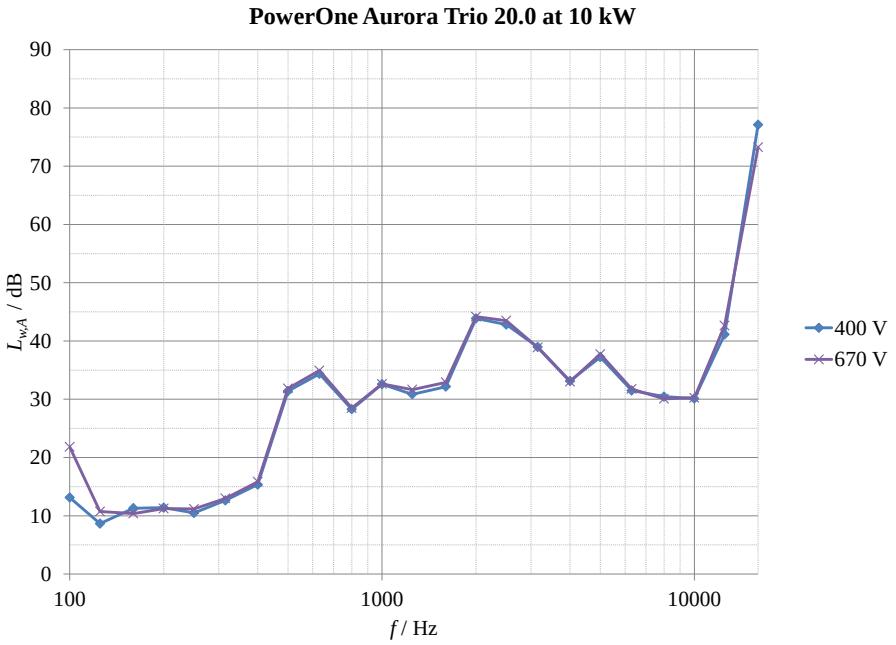

Figure 46: Voltage-related variability of noise emissions of PowerOne Aurora Trio 20.0 at 10 kW.

quency of the mains grid (and thus the output signal).

PowerOne PVI-3.0 (Figure 47) exhibits a near-uniform decrease of noise emis-

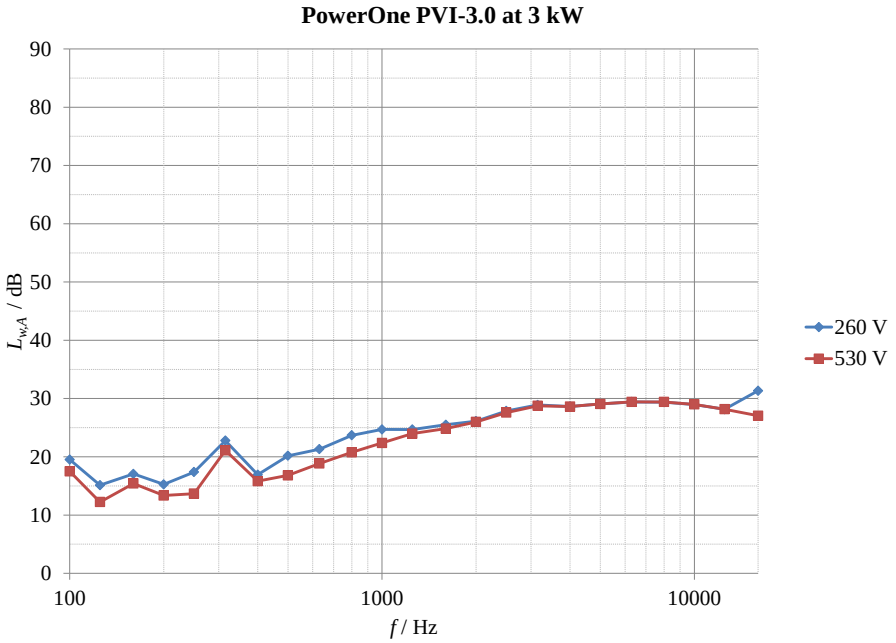

Figure 47: Voltage-related variability of noise emissions of PowerOne PVI-3.0 at 3 kW.

sions with increasing voltage, again suggesting a current-dependent increase in noise.

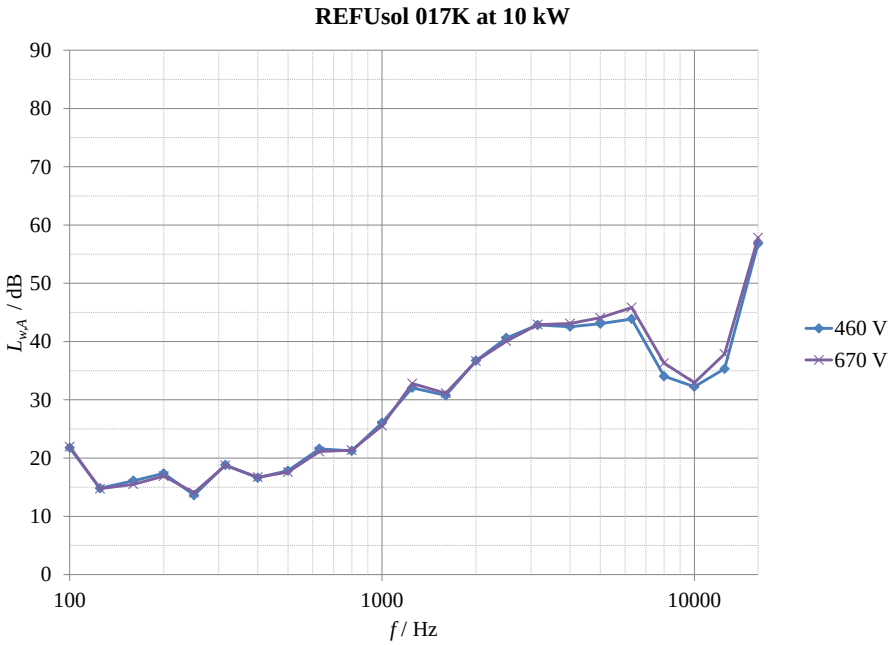

Figure 48: Voltage-related variability of noise emissions of REFUsol 017K at 10 kW.

REFUsol 017K (Figure 48) exhibits no variations in noise output due to voltage, aligning itself with the Kostal device.

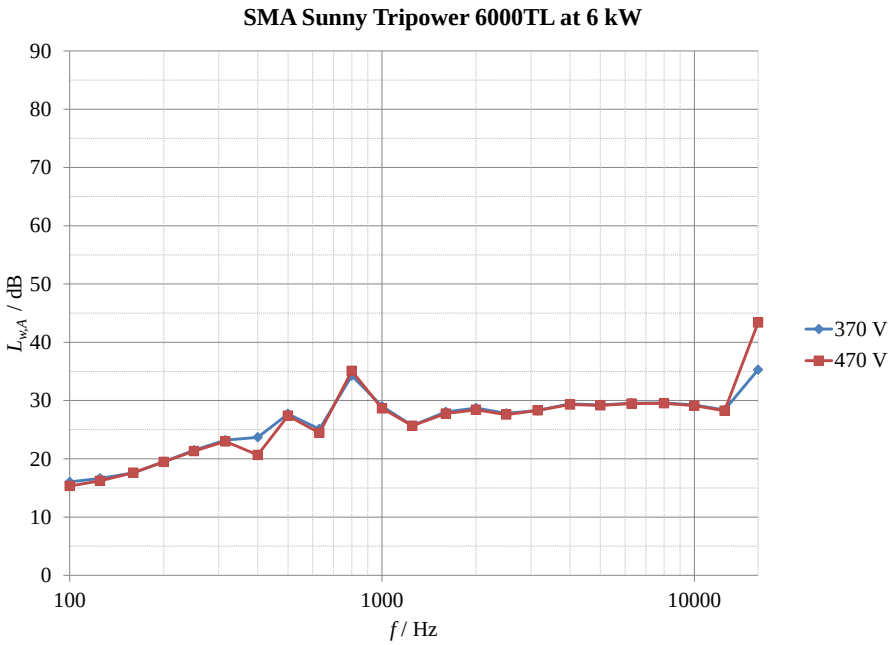

Figure 49: Voltage-related variability of noise emissions of SMA Sunny Tripower 6000TL at 6 kW.

SMA Sunny Tripower 6000TL (Figure 49) exhibits no significant variations due to voltage on the lower frequencies; however, there is a significant voltage-related increase at the switching frequency on the 16 kHz band.

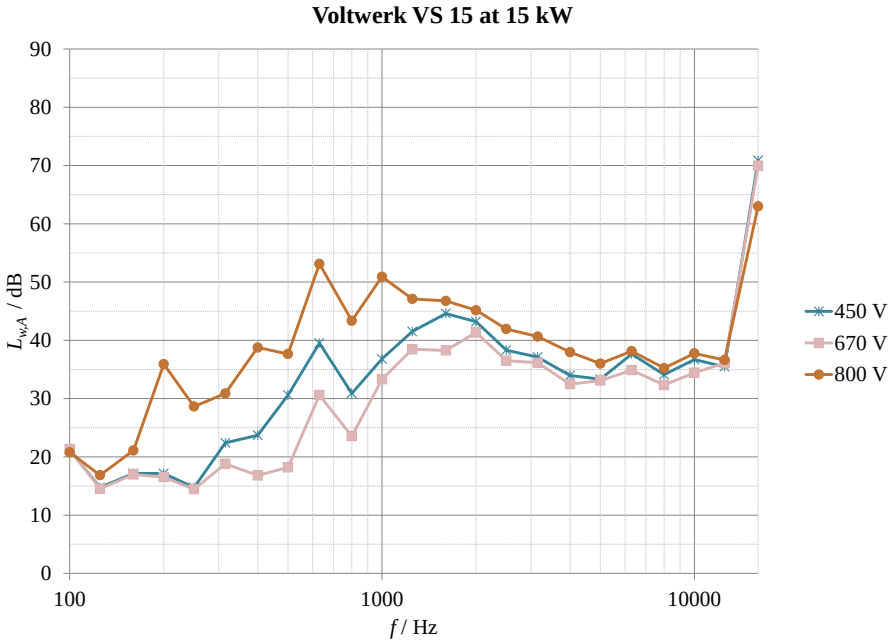

Figure 50: Voltage-related variability of noise emissions of Voltwerk VS 15 at 15 kW.

Voltwerk VS 15 (Figure 50), then again, is all over the place. Low-frequency noise first drops as voltage increases from 450 V to 670 V, and then increases significantly as the voltage rises further to 800 V. On the 16 kHz band, there is a slight, but significant decrease in noise emission with increasing voltage. The eccentric behaviour of noise emissions on low frequencies might be explained by an adaptable fan speed control mechanism, where the device heated significantly between the measurements at 670 and 800 V. This would increase airflow, and thus fan-related noise. The decrease from 450 to 670 V, then, could be explained by a current-related increase in noise emission at low frequencies. However, this is not in line with the measurements conducted on the Generic Device choke array. There is, nevertheless, a possibility that the electrical configuration of the Voltwerk device differs significantly enough to merit speculation on this seemingly erratic behaviour.

Altogether, there is no conclusive evidence to support any universal conclusions regarding voltage-related variability in noise emissions. Low frequency sound emissions rose in two of the eight devices, decreased in one, remained unchanged in four and behaviour was erratic in one. High frequency emissions increased with voltage in two devices, decreased in three devices, and remained unchanged in two devices. Therefore, it is possible that voltage-related variations in noise emissions are dependent also on the electrical configuration of the device.

7.3.3 Power-related variability of noise emissions

Of the measured devices, Fronius IG TL 5.0, PowerOne PVI-3.0 and SMA Sunny Tripower 6000TL were run at only one power rating, thus invalidating them from power-based analysis.

Danfoss TLX 15 (Figure 51) displays prominent increases in low-frequency noise due to increasing power, lending to the conclusion that there exists an adjustable-speed fan and some form of fan speed control. There is also a prominent rise at the 16 kHz band, also suggesting current-based increases in noise output as was suggested in the study of voltage-related variability.

Kostal PIKO 8.3 (Figure 52) displays similar behaviour, with both low- and high-frequency emissions increasing with power.

The same pattern is once again repeated on PowerOne Aurora Trio 20.0 (Figure 53).

Similar behaviour is also witnessed in REFUsol 017K (Figure 54).

The pattern is broken in Voltwerk VS 15 (Figure 55), where the device displays similarly erratic behaviour as witnessed in the study of voltage-related variability. Low-frequency emissions first rise up to 10 kW, then drop significantly from 10 kW

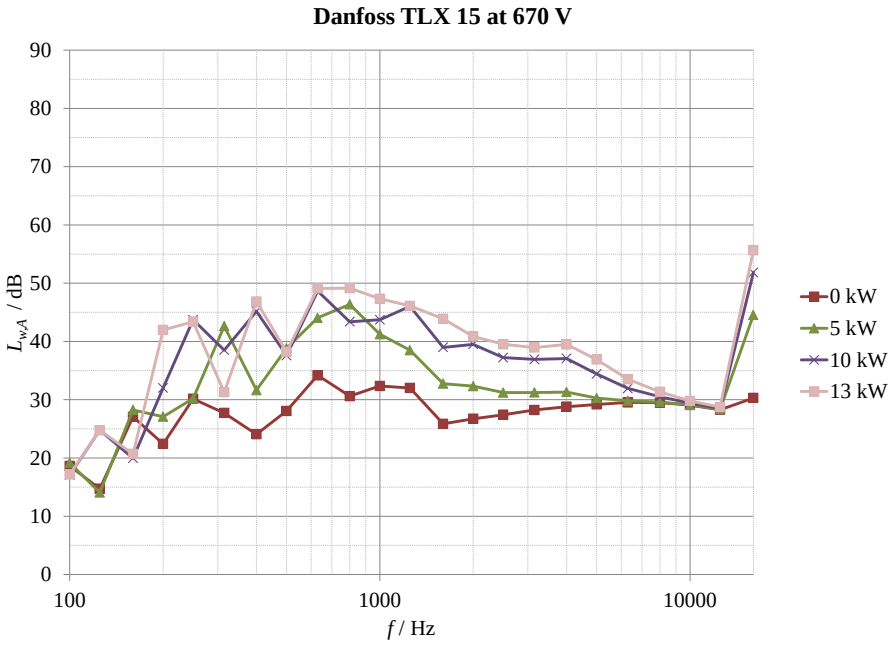

Figure 51: Power-related variability of noise emission of Danfoss TLX 15 at 670 V.

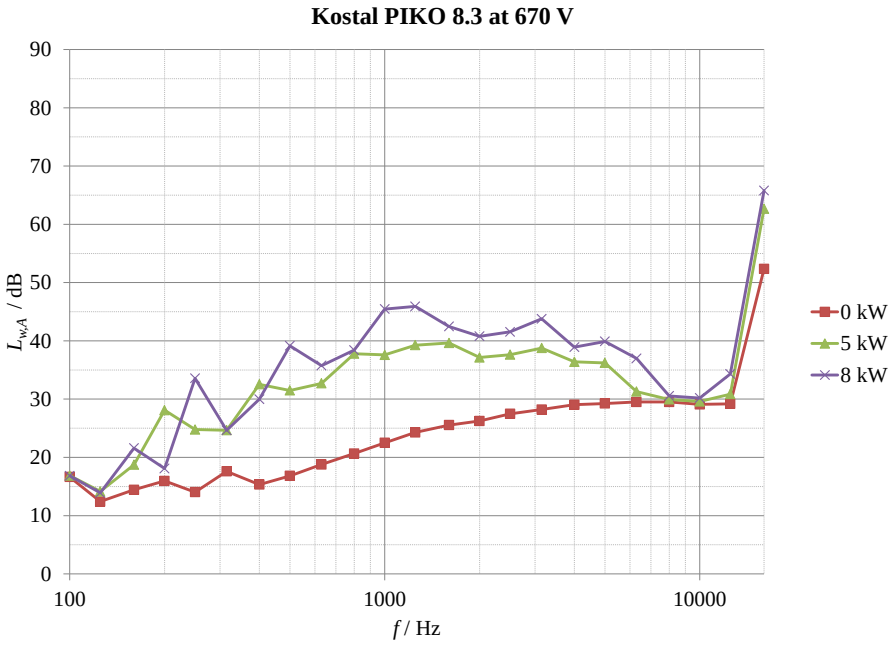

Figure 52: Power-related variability of noise emissions of Kostal PIKO 8.3 at 670 V.

to 15 kW. High-frequency noise emissions also behave mystically, first rising significantly from 0 kW to 5 kW, then dropping from 5 kW to 10 kW, and then again rising remarkably from 10 kW to 15 kW. All in all, Voltwerk VS 15 exhibits somewhat mystifying characteristics of noise emissions in relation to both voltage and

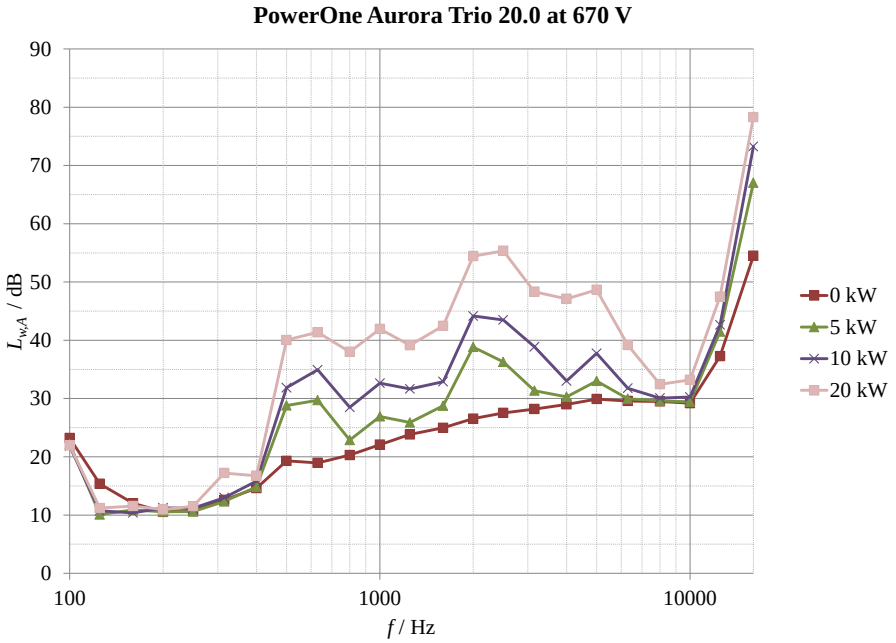

Figure 53: Power-related variability of noise emissions of PowerOne Aurora Trio 20.0 at 670 V.

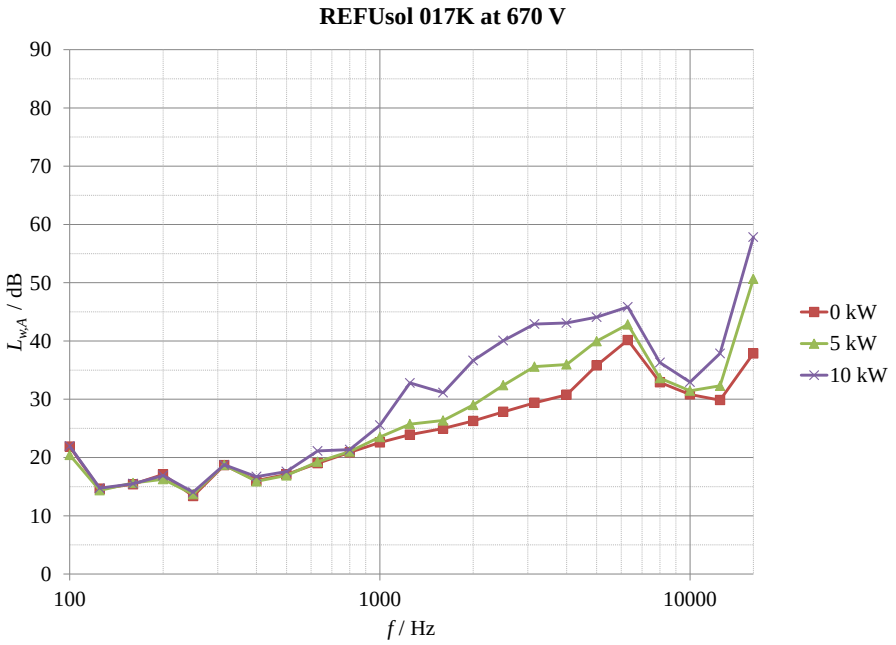

Figure 54: Power-related variability of noise emissions of REFUsol 017K at 670 V.

power. However, both abnormalities seem to be related to the measurements at the operating point of 670 V at 15 kW. It is therefore possible that this inconsistency is due to simple measurement error. Further measurements are warranted to determine whether this is the case.

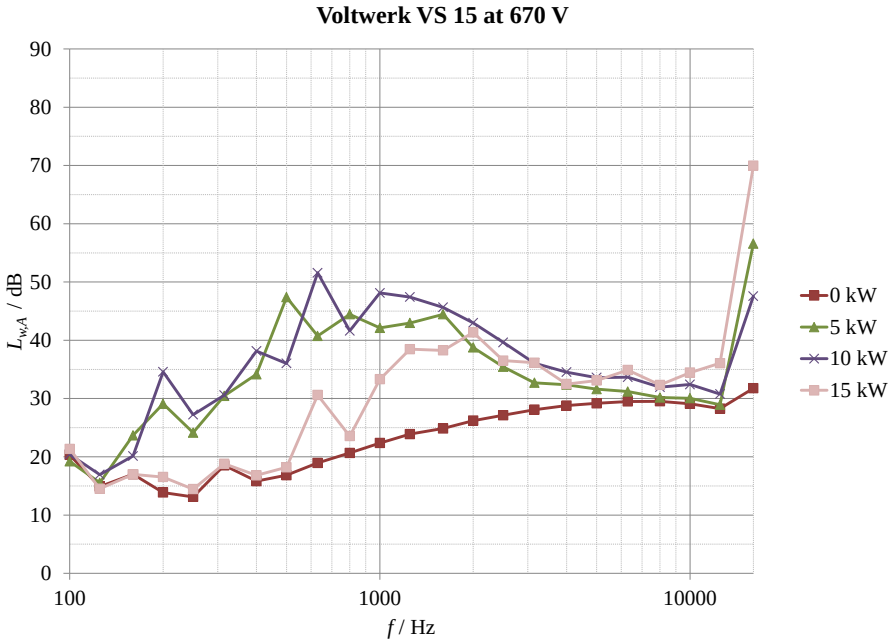

Figure 55: Power-related variability of noise emissions of Voltwerk VS 15 at 670 V.

Summing up, with the exception of one device, all measured devices showed positive correlations of noise emissions with power both at low and high frequencies. Low-frequency noise is explained readily by increased fan speeds due to need for increasing heat dissipation, suggesting functioning fan speed control in all measured devices. High-frequency noise can be explained by increased currents in the choke assembly causing increasing magnetostriction.

8 Conclusions and suggestions

The aim of this thesis was to answer these questions:

1. What are typical noise emission levels of on-market solar inverters?
2. Do these devices' noise emissions exhibit variations due to different voltage or power levels?
3. How much noise is due to the cooling fans, how much due to chokes, and how much due to everything else?

It was found, that the noise emissions of solar inverters exhibit significant variation, with no clear tendencies regarding variability due to operating voltage. However, there was a clear tendency for noise emissions to rise with increasing power when this observation was restricted to a particular device. No such tendency arose when comparing rated power and noise emissions across different devices. The tested devices ranged from essentially soundless to roaring death machines from hell.

It was clear from the measurements, that most, if not all, noise emissions below 10 kHz are due to the cooling fans. The rise in airflow requirements explains the rise of noise emissions in those devices where a variable-speed cooling fan is employed.

The noise emissions above 10 kHz, on the other hand, seem to indicate noise emissions from chokes. There are slight emissions at above 10 kHz from sources other than chokes, but these border on meaningless when compared to the emissions due to the chokes. The emissions of the chokes show no clear relationship with operating voltage or power, suggesting instead that high-frequency noise is dependent on both the voltages and currents of the device and the electrical topology of the device.

The significance of noise emissions from the choke versus the cooling fan also displays a range of results. The inclusion of the 16 kHz octave band (seen here as representative of choke noise) caused a rise of between 1.0 dB and 23.5 dB in the total noise emission. In no devices was the total noise emission unchanged. Thus, it can be concluded that high-frequency noise is a significant contributor to total noise emissions.

High-frequency noise is, nevertheless, not included in the presentation of noise emission figures of on-market devices. This represents a significant distortion of actual noise emissions. An effort should be made to alter the measurement process to yield more representative results.

8.1 Suggestions for noise emission declarations for solar inverters

It was shown that for this family of devices, the standard procedure outlined in ISO 3744 is insufficient to appropriately represent the total noise emission. Thus, the author of this thesis proposes that solar inverters, and frequency converters in general, should follow the guidelines outlined in ISO 7779, ISO 9295 and ISO 9296. The suggested method is the expansions of the measurement bandwidth up to 20 kHz. This represents truer picture of the total noise emission, without the added confusion of having to interpret multiple noise emission figures for the same operating point.

The determination of emission sound pressure values via ISO 11203 proved to be a poor choice. Surface non-uniformity indices for noise emissions, particularly for higher frequencies, were high: frequently exceeding 6 dB. Thus, it is concluded that an observer position need be determined, and emission sound pressure levels should be determined empirically via ISO 11201, as suggested by ISO 7779. Computational determination of sound pressure levels utterly fails the assumption that sound power is distributed evenly across an enveloping surface.

Thus, it is suggested that for this family of devices, measurements should be conducted to determine

- A-weighted sound power level $L_{W,A}$ on the frequency band 100 Hz–20 kHz (ISO 3744 is recommended)
- A-weighted emission sound pressure level $L_{p,A}$ at the operator position on the same frequency band (ISO 11201 is recommended)
- Both quantities in the idling condition and in the full power condition

8.2 Suggestions for dealing with cooling fan and choke noise

The most obvious course of action for the immediate reduction of fan noise emission is the implementation of fan speed control. The reductions by this course of action are especially significant at frequencies below the modulation frequency. This reduces the generation of noise, rather than deal with extant noise.

In dealing with extant noise, it is advisable to explore different configurations for the placement of the fan in the chassis.

Contrary to initial assumptions, it was found that choke noise is mostly airborne rather than structure-borne, and as such, it should be dealt with in the same way as fan noise: alterations in the structures enclosing the sound-radiating object.

Since both fan and choke noise are essentially sources of airborne sound, it might be feasible to explore different types of enclosures for either noise source within the devices themselves.

8.3 Suggestions for further research

Further research needs to be conducted on the electromagnetic generation of noise in chokes. Both voltage- and power-related variations in noise emissions need to be elucidated to a greater extent. The author proposes that a measurement series with a finer gradation in both power and voltage be conducted to explore the causal mechanisms that relate current, voltage and power to acoustic noise emissions.

Furthermore, the idling artefact needs to be explored. Although it is not a significant contributor to total noise, it was not observed in the case where the cooling fan was disabled. Thus, the measurement series was incomplete, and it should be explored whether this component reaches significance when the cooling fan is off.

References

Backman, J. 2005. *Akustiikka ja äänen fysiikka.* Course material for HUT course S-89.3310 Acoustics and the physics of sound.

Backman, J. 2008. *Sähköakustiikka.* Course material for HUT course S-89.3410 Electroacoustics.

Blazev, A. S. 2012. *Photovoltaics for Commercial and Utilities Power Generation.* Fairmont Press, Inc., Lilburn, GA, USA.

Brüel & Kjær. 1996. *Microphone handbook.* Brüel & Kjær, Nærum, Denmark.

Chikazumi, S. 1997. *Physics of Ferromagnetism.* Oxford University Press, New York, NY, USA.

Cremer, L., Heckl, M., and Petersson, B. 2005. *Structure-Borne Sound*, 3rd ed. Springer, Berlin, Germany.

Erkinheimo, H., Käyhkö, K., Niemelä, H., Pullola, E., Saloriutta, J., and Tuomainen, M. 1997. *Taajuusmuuttajat: käyttö, asennus, häiriöt.* Sähköinfo Oy, Espoo, Finland.

Fahy, F. 2001. *Foundations of Engineering Acoustics.* Academic Press, London, UK.

Fukano, T. and Jang, C.-M. 2004. Tip clearance noise of axial flow fans operating at design and off-design condition. *Journal of Sound and Vibration 275,* 3, 1027–1050.

Gérard, A., Berry, A., and Masson, P. 2005. Control of tonal noise from subsonic axial fan. Part 1: reconstruction of aeroacoustic sources fromo far-field sound pressure. *Journal of Sound and Vibration 288,* 4, 1049–1075.

Hongisto, V. 2007. *Meluntorjunta.* Course material for HUT course S-89.3470 Noise control.

IEC 60942. 2003. *Electroacoustics — Sound calibrators.* IEC, Geneva, Switzerland.

IEC 61043. 1993. *Electroacoustics — Instruments for the measurement of sound intensity — Measurement with pairs of pressure sensing microphones.* IEC, Geneva, Switzerland.

IEC 61094. 2000. *Electroacoustics — Measurement microphones.* IEC, Geneva, Switzerland.

IEC 61260. 1995. *Electroacoustics — Octave-band and fractional-octave-band filters.* IEC, Geneva, Switzerland.

IEC 61672. 2000. *Electroacoustics — Sound level meters.* IEC, Geneva, Switzerland.

ISO 11200. 2009. *Acoustics. Noise emitted by machinery and equipment. Guidelines for the use of basic standards for the determination of emission sound pressure levels at a work station and other specified positions.* ISO, Geneva, Switzerland.

ISO 11201. 2010. *Acoustics. Noise emitted by machinery and equipment. Determination of emission sound pressure levels at a workstation with negligible environmental corrections.* ISO, Geneva, Switzerland.

ISO 11202. 2010. *Acoustics. Noise emitted by machinery and equipment. Determination of emission sound pressure levels at a workstation applying approximate environmental corrections.* ISO, Geneva, Switzerland.

ISO 11203. 2009. *Acoustics. Noise emitted by machinery and equipment. Determination of emission sound pressure levels at a workstation from the sound power level.* ISO, Geneva, Switzerland.

ISO 11204. 2010. *Acoustics. Noise emitted by machinery and equipment. Determination of emission sound pressure levels at a workstation applying accurate environmental corrections.* ISO, Geneva, Switzerland.

ISO 11205. 2009. *Acoustics. Noise emitted by machinery and equipment. Determination of emission sound pressure levels at a workstation using sound intensity.* ISO, Geneva, Switzerland.

ISO 12001. 1996. *Acoustics. Noise emitted by machinery and equipment. Rules for the drafting and presentation of a noise test code.* ISO, Geneva, Switzerland.

ISO 226. 1987. *Acoustics – Normal equal-loudness level contours.* ISO, Geneva, Switzerland.

ISO 3740. 2000. *Acoustics – Determination of sound power levels of noise sources – Guidelines for the use of basic standards.* ISO, Geneva, Switzerland.

ISO 3741. 1999. *Acoustics – Determination of sound power levels of noise sources using sound pressure – Precision methods for reverberation test rooms.* ISO, Geneva, Switzerland.

ISO 3744. 2010. *Acoustics – Determination of sound power levels of noise sources using sound pressure – Engineering methods for an essentially free field over a reflecting plane.* ISO, Geneva, Switzerland.

ISO 3745. 2003. *Acoustics – Determination of sound power levels of noise sources using sound pressure – Precision methods for anechoic and hemi-anechoic rooms.* ISO, Geneva, Switzerland.

ISO 3746. 2010. *Acoustics – Determination of sound power levels of noise sources using sound pressure – Survey method using an enveloping measurement surface over a reflecting plane.* ISO, Geneva, Switzerland.

ISO 3747. 2010. *Acoustics – Determination of sound power levels of noise sources using sound pressure – Engineering survey methods for use in situ in a reverberant environment.* ISO, Geneva, Switzerland.

ISO 4871. 1996. *Acoustics – Declaration and verification of noise emission values of machinery and equipment.* ISO, Geneva, Switzerland.

ISO 6926. 2000. *Acoustics – Requirements for the performance and calibration of reference sound sources used in the determination of sound power levels*, Second, corrected and reprinted ed. ISO, Geneva, Switzerland.

ISO 7779. 2010. *Acoustics – Measurement of airborne noise emitted by information technology and telecommunications equipment.* ISO, Geneva, Switzerland.

ISO 9295. 1989. *Acoustics – Measurement of high frequency noise emitted by computer and business equipment*, First, corrected and reprinted ed. ISO, Geneva, Switzerland.

ISO 9296. 1988. *Acoustics – Declared noise emission values of computer and business equipment.* ISO, Geneva, Switzerland.

ISO 9614. 1993-2002. *Acoustics – Determination of sound power levels of noise sources using sound intensity.* ISO, Geneva, Switzerland.

John J. Winders, J. 2002. *Power Transformers – Principles and Applications.* Marcel Dekker Inc., New York, NY, USA.

Krell, C., Baumgartinger, N., Krismanic, G., Leiss, E., and Püfner, H. 2000. Relevance of multidirectional magnetostriction for the noise generation of transformer cores. *Journal of Magnetism and Magnetic Materials 215–216*, 634–636.

Lahti, T. 1995. Akustinen mittaustekniikka. Course material for HUT course S-89.3430 Acoustic measurement technology.

Lahti, T. 2009. Teknistä akustiikkaa pähkinänkuoressa. In *Akustiikkapäivät 2009.* Akustinen seura, Espoo, Finland.

Maaloum, A., Koudiri, S., Bakir, F., and Rey, R. 2003. Effect of inlect duct contour and lack thereof on the noise generated of an axial flow fan. *Applied Acoustics 64,* 10, 999–1010.

Niiranen, J. 1999. *Sähkömoottorikäytön digitaalinen ohjaus*, 2nd ed. Otatieto, Helsinki, Finland.

Otto, S., Nielsen, J. S., Olesen, K., Jensn, B. B., Kristensen, H. J., Breitzke, B., Hansen, T., and Sørensen, J. K. 2006. *Practical thermal management.* Tech. rep., Sammenslutningen for Pålidegheds- og Miljøteknik.

Quinlan, D. and Bent, P. 1998. High frequency noise generation in small axial flow fans. *Journal of Sound and Vibration 218,* 2, 177–204.

Shireen, W., Kulkarni, R. A., and Arefeen, M. 2006. Analysis and minimization of input ripple current in PWM inverters for designing reliable fuel cell power systems. *Journal of Power Sources 156,* 2, 448–454.

Tanttari, J. and Saarinen, K. 1995. *Työkeneiden melun vähentäminen – perusteet.* Tech. rep., Metalliteollisuuden keskusliitto, Tampere, Finland.

Thorborg, K. 1988. *Power electronics.* Prentice Hall International Ltd, Cambridge, UK.

Weiser, B., Pfützner, H., and Anger, J. 2000. Relevance of magnetostriction and forces for the generation of audible noise of transformer cores. *IEEE Transactions on Magnetics 36,* 5, 3759–3777.